Aus dem Zentrum für klinische Tiermedizin
der Tierärztlichen Fakultät der
Ludwig-Maximilians-Universität München

Arbeit angefertigt unter der Leitung von Univ.- Prof. Dr. R. Wanke

Clinical and pathomorphological characterization of uninephrectomized GIPR^{dn} transgenic diabetic mice

Inaugural-Dissertation
zur Erlangung der tiermedizinischen Doktorwürde
der Tierärztlichen Fakultät der
Ludwig-Maximilians-Universität München

von Nicole Barbara Ryba
aus Genf

München 2011

Gedruckt mit der Genehmigung der Tierärztlichen Fakultät
der Ludwig-Maximilians-Universität München

Dekan:	Univ.-Prof. Dr. Braun
Berichterstatter:	Univ.-Prof. Dr. Wanke
Korreferent:	Univ.-Prof. Dr. Kaspers

Tag der Promotion: 12. Februar 2011

Table of contents

1. Introduction

The prevalence of diabetes mellitus has taken on epidemic proportions and is increasing continuously. In 2009, more than 220 million people were diagnosed with diabetes worldwide (WHO 2009). It is estimated that approximately 285 million people, aged 20-79 years, will be diagnosed with diabetes worldwide in 2010. By 2030, the figure is expected to rise to 439 million of the adult population (IDF 2006).
Although great advances have been made in the care of patients with diabetes, it's still long before all patients suffering from diabetes mellitus reach the therapeutic goal and long term damages are confined (Kerner 1998).
In most countries, diabetes is one of the major causes of premature illness and death. Over time it leads to serious damage to many of the body's organ systems induced by macro- and microvascular disease. Cardiovascular disease causes the death of at least 50% of people with diabetes, depending on the population.
One of the most important sequella in chronic diabetes is diabetic nephropathy. When diabetic nephropathy progresses it eventually leads to end stage renal disease (ESRD). 26 million American adults suffer from diabetic nephropathy (2010 National Kidney Foundation). In Germany, diabetes mellitus is the underlying disease in 23% of all patients suffering from ESRD and 34% of patients with renal disease add to this list every year (www.bundesverband-niere.de/files/QuaSi-Niere-Bericht_2006-2007).
To this day, the pathogenesis of diabetic nephropathy hasn't entirely been investigated.
Understanding the basic biology of diabetes mellitus and associated late complications required the adoption of rodent models. The observation of e.g. humanized, transgenic or knock-out mouse models provided an important innovation in diabetes research. Further, selective inbreeding has produced several animal strains that are considered reasonable models of Type 1 and Type 2 diabetes mellitus and related phenotypes such as obesity and insulin resistance (Rees and Alcolado, 2005). A novel animal model of diabetic kidney disease are transgenic mice expressing a dominant negative glucose-dependent insulinotropic polypeptide receptor ($GIPR^{dn}$), which develop kidney lesions that resemble those observed in human diabetic patients (Herbach et al., 2009). In addition, necropsy of a $GIPR^{dn}$ transgenic mouse by coincidence revealed unilateral renal agenesia. The remaining kidney of this animal showed advanced diabetes-associated glomerular and tubulo-

interstital lesions that were more severe than kidney alterations of GIPR^{dn} transgenic animals investigated so far (Wanke and Herbach, personal communication).

In the present study, uninephrectomy was performed in young GIPR^{dn} transgenic mice, in order to mimic the situation observed in the animal that exhibited unilateral renal agenesia. A precise clinical, pathomorphological and quantitative stereological survey was performed in uninephrectomized GIPR^{dn} transgenic mice to characterize kidney lesions in comparison to their non-transgenic and sham operated counterparts.

2. Literature review

2.1 Diabetes mellitus

2.1.1 Definition and description of diabetes mellitus

Diabetes mellitus is defined as a regulatory dysfunction of metabolism, mainly characterized by hyperglycemia. The causes of diabetes are multiple whereby both genetic and environmental factors play major roles in its etiology. The underlying cause of diabetes mellitus may be destruction of the ß-cells of the pancreas leading to impaired insulin secretion, diminished effectiveness of insulin on target tissues, or both. The deficient action of insulin induces abnormalities of the carbohydrate, fat and protein metabolism. Chronic hyperglycemia leads to long-term damage, dysfunction and failure of multiple organs, primarily the eyes, kidneys, nervous system, heart, brain and peripheral arteries (Kerner 1998). If the metabolic abnormality is mild, patients may be asymptomatic, while in the presence of overt hyperglycemia, characteristic symptoms, such as thirst, polydipsia, polyuria, and weight loss often occur. Diabetic ketoacidosis and the non-ketotic hyperglycemic-hyperosmolar dehydration-syndrome are acute life-threatening situations, and there is an increased mortality associated with diabetes induced cardiovascular and end-stage renal disease (ESRD). Diabetes mellitus type 1 and type 2 are the most common types of diabetes mellitus in humans, whereas gestational diabetes and a few other forms of diabetes mellitus play a secondary role. Diabetes mellitus type 1 is an insulin dependent condition with its onset usually in childhood or before the age of 25, as opposed to diabetes mellitus type 2 with its onset after middle age and a primarily non insulin dependent disposition. Type 1 diabetes mellitus is characterized by destructive lesions of pancreatic cells either by an autoimmune mechanism or of unknown cause. Type 2 diabetes is distinguished by combinations of decreased insulin secretion and decreased insulin sensitivity (insulin resistance) (Kuzuya et al., 2002).

2.1.2 Diagnosis of diabetes mellitus

Urine Test

The Dipstick test is a very simple color test to ascertain the presence of glucose in the urine. However, dipstick tests are not confirming enough to use them as a definite diagnosing tool. The reasons are for example that the results can be easily misinterpreted, other ketonic or aldehydic groups can interfere with the results, and it is a quite costly test. Anyhow, this is a quick way of finding out the disease at a household level (www.DiabetesMellitus-Information.com, 2006).

Blood tests

In the absence of a more specific biological marker to define diabetes, venous plasma glucose measurement remains the foundation of diagnostic criteria.

The diagnosis is made on the basis of fasting blood glucose levels.

If casual plasma glucose concentrations exceed 200 mg/dl, diabetes mellitus is diagnosed. Glucose levels above 100 mg/dl require fasting blood glucose tests. If fasting glucose concentrations of at least 126 mg/dl are obtained twice, diabetes mellitus is diagnosed. Fasting glucose levels between 100 and less than 126 mg/dl are referred to as „impaired fasting glucose“ (IFG). When receiving glucose concentrations between 90 and 99 mg/dl, the diabetic risk factors should be observed (Kerner et al., 2004).

Glucose tolerance test

With fasting plasma glucose concentrations between 100 and 125 mg/dl, a glucose tolerance test is indicated. The oral glucose tolerance test (OGTT) is an important instrument for identifying the pre-diabetic metabolic state in humans. After oral intake of 75 g glucose, the blood glucose level is determined at intervals of 60 and 120 minutes. If blood glucose levels exceed 200 mg/dl after 120 minutes, diabetes mellitus is diagnosed. Plasma glucose concentrations between 140 and below 200 mg/dl two hours after glucose intake indicate impaired glucose tolerance (IGT) (Kerner et al., 2004).

2.1.3 Classification of diabetes mellitus

Approximately 90% of the people suffering from diabetes mellitus are diagnosed with type 2 diabetes. Unlike type 1 diabetes, the onset of type 2 diabetes is usually found after middle age (40 years), and more often at age 60 (IDF 2006).

In 1997, the conventional classification of the different diabetes mellitus types was discarded, due to the fact that it did not describe the pathogenetic mechanisms, but rather the therapy applied. The ADA introduced a new nosological classification for diabetes mellitus, thus, distinguishing type 1 diabetes, type 2 diabetes, other specific diabetes types and gestational diabetes (Kerner 1998).

Table 1 shows the recent nosological classification.

Table 1 Classification of diabetes mellitus

I. Type 1 diabetes mellitus (destruction of β-cells causing absolute insulin dependency)
- A. immunologic
- B. idiopathic

II. Type 2 diabetes mellitus (Insulin resistance and/ or failure of β-cell secretion)

III. Other forms of diabetes mellitus
- A. Genetic disorders in β-cell function e.g.
  (chromosome 12, HNF-1 α (formerly MODY 3), chromosome 7, glucokinase (formerly MODY 2), chromosome 20, HNF-4 α (formerly MODY 1), mitochondrial DNA)
- B. Genetic disorders in insulin effect
  (Type A insulin-resistance, leprechaunism, Rabson-Mendenhall-syndrome, lipatrophic diabetes)
- C. disease of the exocrine pancreas
  (pancreatitis, trauma/ pancreatectomy, neoplasia, cystic fibrosis, hemo-chromatosis, calcifying fibrotic pancreopathy)
- D. Endocrinopathies
  (acromegaly, Cushing-syndrome, glucagonoma, pheochromocytoma, hyperthyroidism, somatostatinoma, aldosteronoma)
- E. Diabetes-forms induced by medication or chemicals
  (neuroleptika (in particular Clozapin, Olanzapin), Pentamidin, Niacin, glucocorticoids, hormones of the thyroid, Diazoxid, β-adrenergic agonists, Thiazide, Phenytoin, α-interferon)
- F. Infections
  (congenital rubella syndrome, cytomegalovirus infection)
- G. Uncommon forms of immunomediated diabetes mellitus
  („stiff-person“-syndrome, Anti-insulin-receptor-antibody)
- H. Other genetic syndromes, likely to be associated with diabetes mellitus
  (Down-syndrome, Klinefelter-syndrome, Turner-syndrome, Wolfram-syndrome, Friedreich-ataxia, Laurence-Moon-Biedl-syndrome, Chorea huntington, dystrophia myotonica, porphyria, Prader-Willi-syndrome)

IV. Gestational diabetes

2.1.4 Epidemiology

In 2010, it is estimated that 6.6% of adults aged 20-79 years worldwide are diagnosed with diabetes mellitus, and this number is continuously rising (IDF 2006). The underlying cause of diabetes is to some extent a genetic predisposition. Since the genetic distribution hasn't changed during the years, it is clear that trigger factors play a major role in the development of diabetes. These factors include population growth, longer life-span, urbanization, unhealthy diet, overweight, obesity, and lack of physical exercise. Without a doubt, diabetes is one of the most challenging health problems in the 21st century and thus a global burden. Unfortunately, the severity of the sequelae is often underrated. In 2006, diabetes was the seventh leading cause of death listed on U.S. death certificates, the cause of death predominantly being end stage renal disease (ADA 2007).

2.2 Diabetic nephropathy

Macroscopically, kidneys of diabetic patients are initially enlarged. This enlargement is mainly the result of a combination of tubular hypertrophy and hyperplasia and interstitial expansion. Diabetic kidneys may also appear normal sized or smaller than kidneys of non-diabetic subjects and these small kidneys are firm and exhibit a granular surface and subcapsular scars (Bilous 2001, Heptinstall 1991).

The clinical syndrome termed 'diabetic nephropathy' is characterized by persistent albuminuria, early arterial blood pressure elevation, a relentless decline in glomerular filtration rate (GFR), and a high risk of cardiovascular morbidity and mortality (Parving et al., 2001). Once the clinical manifestations of diabetic nephropathy, including the development of persistent microalbuminuria are present, the structural injury in the kidneys is often already far advanced. There are a variety of alterations involving the kidney, including nodular and diffuse glomerulosclerosis which both can lead to chronic renal failure. The process of diabetic nephropathy in type 1 and type 2 diabetes mellitus is characterized by: increasing microalbuminuria, decreasing glomerular filtration rate, and development or increase of hypertension, and other diabetic-born illnesses (Hasslacher et al., 2009).

Table 2: The stages of diabetic nephropathy – typical findings

Stage	Glomerular filtration	Albuminuria	Blood pressure	Time course (years after diagnosis)
renal hyperfunction	Elevated	Absent	Normal	At diagnosis
clinical latency	High normal	Absent		
Microalbuminuria (insipient nephropathy)	Within the normal range	20-200 µg/min (30-300 mg/day)	rising within or above normal range	5-15
macroalbuminuria or persisting proteinuria	Decreasing	>200 µg/min (>300 mg/day)	Increased	10-15
Renal failure	Diminished	Massive	Increased	15-30

The five stages of diabetic nephropathy modified from (Mogensen et al., 1995)

2.2.1 Glomerular changes

The natural course of diabetic renal disease is thought of as a continuum of glomerular injury.

Diabetic nephropathy is divided into four hierarchical glomerular lesions with a separate evaluation for degrees of interstitial and vascular involvement.

The classification of diabetic glomerulosclerosis is as follows:

Class I, *glomerular basement membrane thickening*: isolated glomerular basement membrane thickening and only mild, nonspecific changes by light microscopy that do not meet the criteria of classes II through IV.

Class II, *mesangial expansion mild (IIa) or severe (IIb*): glomeruli with mild or severe mesangial expansion but without nodular sclerosis (Kimmelstiel-Wilson lesions) or global glomerulosclerosis in more than 50% of glomeruli.

Class III, *nodular sclerosis (Kimmelstiel-Wilson lesions)*: at least one glomerulus with nodular increase in mesangial matrix (Kimmelstiel-Wilson) without changes described in class IV.

Class IV, *advanced diabetic glomerulosclerosis*: more than 50% global glomerulosclerosis with other clinical or pathologic evidence that sclerosis is attributable to diabetic nephropathy (Tervaert et al., 2010).

The earliest morphological alteration in diabetic nephropathy is expansion of the mesangial area. This is caused by an increase in extracellular matrix deposition and mesangial cell hypertrophy. There is a highly significant correlation between glomerular filtration rate and mesangial expansion. Research has shown that high

glucose levels lead to hypertrophy of mesangial cells which is mediated by insulin-like growth-factor I, among other factors (Wolf 2004).

The nodular glomerulosclerosis (*Kimmelstiel-Wilson lesions*) is not as frequently seen as diffuse glomerulosclerosis in diabetes. The nodules are generally associated with some degree of diffuse glomerulosclerosis. Panglomerular glomerulosclerosis (former also called “diffuse” glomerulosclerosis), is characterized by diffuse deposition of basement membrane-like material in the mesangium of the entire glomerulus (Reddi and Camerini-Davalos 1990). Extracellular accumulation of basement membrane components lead to thickening of glomerular and tubular basement membrane and increasing of the mesangial matrix. The structural alterations of the kidney tissue reach from exudative lesions in glomeruli and arterioles to nodular glomerulosclerosis (Wolf 2004).

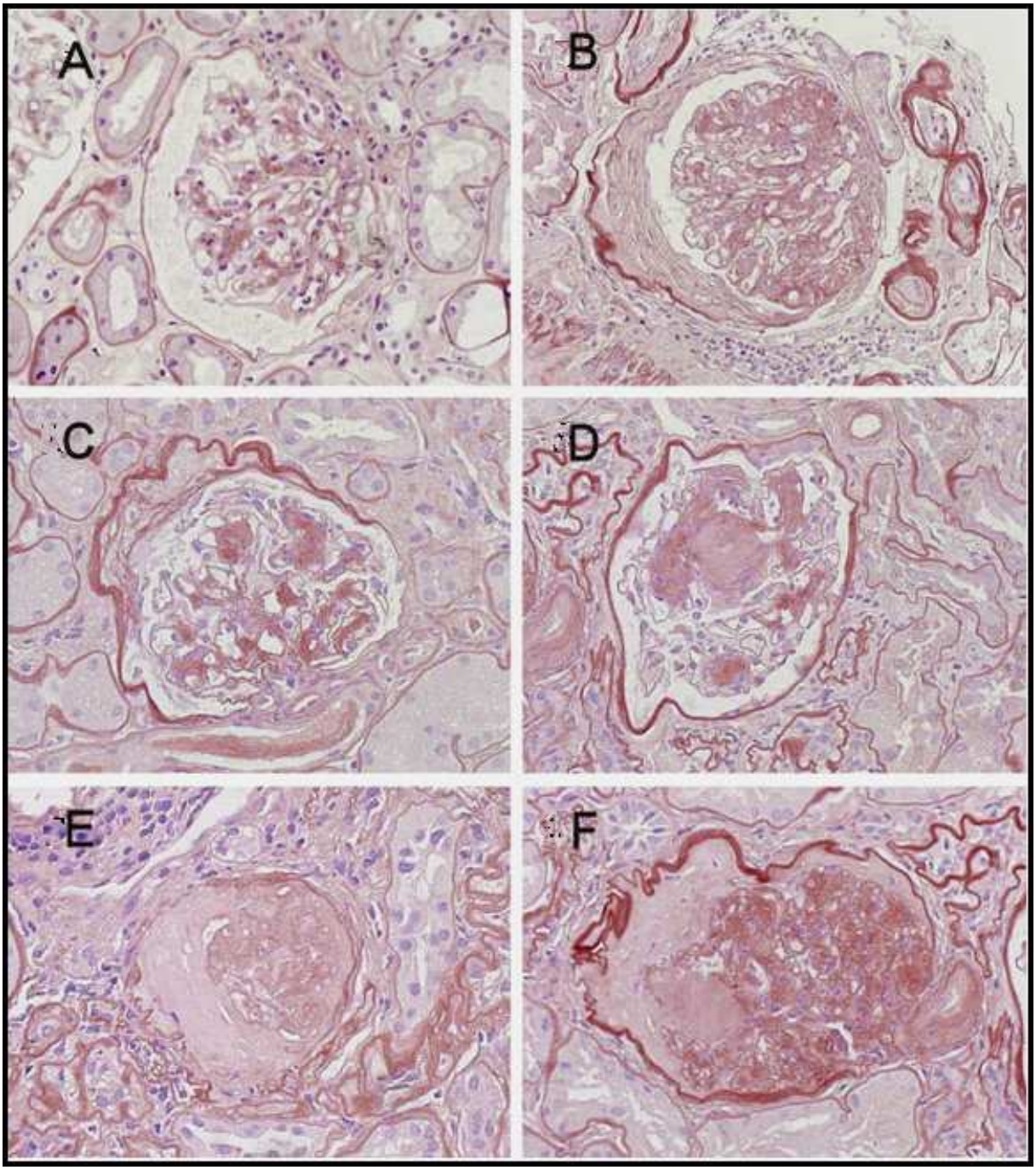

Fig. 1 Diabetic nephropathy in humans modified from: *Pathologic classification of diabetic nephropathy* (Tervaert et al., 2010)

(A, B) Class II glomeruli with mild (A) and moderate (B) mesangial expansion. In panel A, the mesangial expansion does not exceed the mean area of a capillary lumen (IIa), whereas in panel B it does (IIb).

(C, D) In panel D is a class III Kimmelstiel–Wilson lesion. The lesion in panel C is not a convincing Kimmelstiel–Wilson lesion, therefore (on the

basis of the findings in this glomerulus) the finding is consistent with class IIb. For the purpose of the classification, at least one convincing Kimmelstiel–Wilson (as in panel D) needs to be present.

(E) Panel E is an example of glomerulosclerosis that does not reveal its cause (glomerulus from the same biopsy as panel F). For the purpose of the classification, signs of DN* should be histopathologically or clinically present to classify a biopsy with global glomerulosclerosis in >50% of glomeruli as class IV.

(F) In panel F, signs of class IV DN* consist of hyalinosis of the glomerular vascular pole and a remnant of a Kimmelstiel–Wilson lesion on the opposite site of the pole.

* GBM glomerular basement membrane; * DN diabetic nephropathy

2.2.2 Tubular changes

The proximal convoluted segment of the tubules in the diabetic kidney often appears finely vacuolated, with lipid being demonstrable in frozen sections. In more advanced lesions tubular loss, with atrophic tubules showing thickened basement membranes, is obvious. Glycogen deposits in the epithelial cells of the pars recta of the proximal tubule (Armanni-Ebstein lesions), once considered characteristic for diabetes, are recently only occasionally seen (Heptinstall 1991). Furthermore, migration of macrophages and other inflammatory cells into the tubulointerstitium sets in (Ziyadeh and Wolf 2008).

2.2.3 Interstitial changes

In more advanced stages of diabetic nephropathy, tubulointerstitial fibrosis sets in (http://www.diabetes.versorgungsleitlinien.de). The interstitial space is increased as a part of kidney enlargement. Apart from fluid, this space also contains immunologically active cells and fibroblasts. These infiltrates often accompany fibrosis of the interstitial tissues and are thought to contribute to the fibrogenic process (Bilous 2001).

2.2.4 Proteinuria

The morphological changes of the human diabetic kidney are the underlying cause of functional abnormalities, such as proteinuria, with urinary albumin excretion being the most powerful predictor of progression of renal injury (Wang et al., 2000). Proteinuria is no longer simply considered a marker for renal dysfunction, protein is nephrotoxic and thus damages renal tissue (Marshall and Williams 1998). Albumin becomes more toxic to tubular epithelial cells by glycation which explains the great sensitivity of the kidney to proteinuria in diabetes mellitus (Ritz 2006). Circulating macromolecules have to pass through the endothelial fenestrae, the glomerular basement membrane and between podocyte foot processes before appearing in the filtrate, and each of these structures provides both a size and an electrostatic barrier (Bilous 2001). Dysfunction of the glomerular filter and impaired reabsorption of proteins by the epithelial cells of the proximal tubule are two major mechanisms responsible for abnormal urinary excretion of proteins (Camici 2005). Different studies in patients with diabetes mellitus showed an increase in urinary albumin that was above the normal range, but below the level associated with clinical proteinuria in many patients (see Table 2). This subclinical increase in urinary albumin is known as microalbuminuria. Microalbuminuria is the first detectable clinical abnormality in diabetic glomerulopathy. Patients with microalbuminuria are prone to develop established nephropathy, which progresses to end-stage renal failure (Newman et al., 2005). The great medical interest in detecting microalbuminuria lies in the fact that this stage of diabetic nephropathy presents a ‘window of opportunity’: a high renal risk is already indicated by the presence of microalbuminuria, while loss of glomerular filtration rate (GFR) has not yet occurred (Ritz 1999). An additional consequence of overt albuminuria is hypoalbuminemia; this is caused by increased urine albumin excretion which leads to a continuous loss of blood proteins.

2.3. Animal models

2.3.1 Animal models of diabetes mellitus and diabetic kidney disease

Since glomerulosclerosis in diabetic humans is a long term disease and biopsy of the kidney is applied only at the onset of clinical signs of nephropathy, the information received from human patients is solely on more advanced stages of renal dysfunction. Research in this field has leaped forward after Wehner and Petri successfully introduced diabetic animal models in 1983 (Wehner 1983). Consequently, it was possible to study early stages of diabetic nephropathy. The most common animal-models of diabetes mellitus are rodents, in particular mice and rats. When the so-called transgenic technology was developed, it was the mouse which was found to be of great significance as a laboratory animal (Breyer et al., 2005, Wogensen et al., 2005). The selection of an animal model for any type of human disease calls for a specific model that mirrors the human phenotype and, therefore, the clinical suitability of the results. Ideally animal models of diabetes should present the clinical situation of the pathogenesis of diabetes and the resulting organ specific complications, such as diabetic kidney disease. Transgenic mice expressing human genes offer an *in vivo* model for investigation of pathological changes characteristic of diseases in humans (e.g. cells, tissues, immune system) without putting patients at risk. Other advantages of the rodent models are their low initial and relatively low maintenance cost, the possibility of surveying large numbers of animals in a short time, and allowing the study of individuals with precisely known ancestry and the ability to set up back-crosses and matings at will. Also, mice are easily manipulated genetically, enabling the isolation of the influence of single genes (transgenic and knockout mice). On the other hand there are some disadvantages with the rodent models, as well. Renal changes in mice don't resemble those in humans exactly, since rodents can't express the whole clinical picture due to their shorter lifespan. Plus, there are differences in the pathologic processes of the rodent kidney as opposed to the human kidney (Daneshgari et al., 2009).

2.3.1.1 Animal models of type 1 diabetes

Type 1 diabetes mellitus in humans is characterized by a specific destruction of the pancreatic beta cells, commonly associated with immune-mediated damage. Although the damage may occur silently over many years, at clinical presentation there is little surviving beta cell mass and the disorder progresses to absolute insulinopenia. Surgical and toxin-mediated pancreatic damage are valuable tools in the study of the consequences of hyperglycemia in laboratory-animals (Rees and Alcolado 2005).

Streptozotocin-induced diabetic nephropathy in rats

Streptozotocin (STZ) is a naturally occurring chemical that is particularly toxic to the insulin-producing beta cells of the pancreas in mammals and was originally identified in the late 1950s as an antibiotic. Streptozotocin-induced pancreatic injury is commonly used for creating rodent models of type 1 diabetes which develop renal injury with similarities to human diabetic nephropathy. This model can be established in genetically modified rodents for investigating the role of molecular mechanisms and genetic susceptibility in the development of diabetic nephropathy (Tesch and Allen 2007). If administered in a single large dose, streptozotocin can produce diabetes in rodents, probably as a result of direct toxic effects. Alternatively, if multiple small doses of streptozotocin are used (e.g. 40 mg/kg on five consecutive days), this induces an insulinopenic diabetes in susceptible rodents provoked by immune destruction of beta cells, as in human type 1 diabetes. The downside of this method is the risk of the development of kidney tumors (Rees and Alcolado 2005), and interpreting results in this model may be complicated by nonspecific toxicity of STZ (Breyer et al., 2005).

Non-obese diabetic mouse (NOD)

The non-obese diabetic mouse spontaneously develops insulin dependent diabetes mellitus, similar to the illness seen in humans. Insulitis is present when the mice are 4 to 5 weeks old, followed by subclinical beta cell destruction and decreasing circulating insulin concentrations. The pancreatic islets are subjected to an immune attack. Unlike human type 1 diabetes, ketoacidosis is relatively mild. Since these animals have been inbred in laboratories for many generations, many genes and phenotypes will have been enriched, but not all will be relevant to the

pathophysiology of diabetes, either in rodents or in humans (Rees and Alcolado 2005). Disadvantages of the NOD mouse are the unpredictability of the timing of the development of diabetes, and that the NOD mice need insulin therapy to survive long periods (Breyer et al., 2005).

Bio breeding rat (BB)

Development of type 1 diabetes mellitus in the BB rat is associated with features that are shared with human type 1 diabetes mellitus. Disease onset, for example, is preceded by destruction of the insulin-producing beta cells of the pancreas by the immune system, and is controlled by many quantitative trait loci. The BB rat shows hyperglycemia and vascular complications arising from suboptimal control of blood glucose levels (Yang and Santamaria 2006). In these diabetic rats, weight loss, polyuria, polydipsia, hyperglycaemia and insulinopenia develop at around 12 weeks of age. In common with the human disease, ketoacidosis is severe and fatal unless exogenous insulin is administered (Rees and Alcolado 2005).

Long Evans Tokushima lean rat (LETL)

Diabetes mellitus in Long-Evans Tokushima Lean (LETL) rats closely resembles type 1 diabetes in humans, although the prevalence of diabetes is only approximately 20% in these rats. Two sub-strains from the original inbred LETL rat were established, a diabetes-prone (KDP) and a non-diabetic (KND) strain. The features of KDP rats are a high incidence of diabetes (over all approximately 70%) (Komeda et al., 1998).

New Zealand white rabbit

Through successive inbreeding a colony of rabbits was developed showing a spontaneous onset of diabetes mellitus. The diabetic animals are not obese. Despite marked increases in serum and urinary glucose, only mild ketonemia is observed (Roth and Conaway 1982).

Keeshond dog

The Keeshond dog comes from a line of dogs with an inherited condition causing them to become spontaneously diabetic at the age of 2-6 months, but not obese. Aplasia of beta cells of the islet of Langerhans is evident at birth and causes

insulinopenia. Persisting solitary β-cells produce sufficient insulin to maintain growth until the body's insulin requirement exceeds insulin produced, and the onset of diabetes mellitus occurs (Kramer 1981).

Chinese hamster

Inbred lines of the Chinese hamster develop an insulin-deficient, nonobese form of diabetes mellitus type 1 (Kempe et al., 1993). There are six inbred sublines of Chinese hamsters that have greater than 85% incidence of glucosuria. At birth, hamsters from inbred sublines are considered prediabetic, later on they develop diabetes ranging from mild to severe. Morphologic changes have been observed in pancreatic islets, kidney, nerve, blood vessels, eyes, brain, and genito-urinary systems of diabetic Chinese hamsters. Pathogenesis of diabetes mellitus in this animal appears to be related to an increased demand for insulin. Initially there is a positive response to this demand by beta cells, but exhaustion occurs. This is followed by a decrease in beta cell mass and relative or absolute insulin deficiency (Gerritsen 1982). The diabetic Chinese hamster may be a valuable experimental model for studying the metabolic abnormalities of a genetic diabetic syndrome not easily measured in humans *in vivo* (Frankel et al., 1974).

2.3.1.2 Animal models of type 2 diabetes

Type 2 diabetes represents a heterogeneous group of medical conditions characterized by insulin resistance and impaired insulin secretion and defined by a raised fasting or post-challenge blood glucose. But, for many patients with diabetes mellitus type 2, several genetic and environmental factors contribute to the origin and progression of the disease and the late complications. Animal models of type 2 diabetes are likely to be as complex and heterogeneous as the human condition. However, many of the strains used today have been generated by selective inbreeding of animals that spontaneously develop a type 2 diabetes-like phenotype.
Studying these different animal models may help explain why some people with pathological obesity never develop type 2 diabetes whilst others become hyperglycemic at relatively moderate levels of insulin resistance and obesity (Rees and Alcolado 2005).

Goto Kakisaki rat (GK)

The Goto Kakisaki rat is a genetic model of type 2 diabetes mellitus. Mildly glucose-intolerant Wistar rats were selectively inbred to achieve this rat model. The adult GK rat displays decreased beta cell mass together with mild hyperglycemia, glucose intolerance, impaired glucose-induced insulin secretion, hepatic glucose overproduction, and moderate insulin resistance. Impaired development of the GK rat pancreas probably results from insufficiency of extra-pancreatic factors necessary for the growth and survival of fetal pancreatic cells (Miralles and Portha 2001). The fasting blood glucose is only mildly elevated but rises further when glucose is administered. The complications of diabetes seen in humans can be compared with some features represented by the GK rat. These include renal lesions, structural changes in peripheral nerves and abnormalities of the retina. Research into these phenomena demonstrates another example of how animal experimentation gives way to fields that could not be easily studied in human beings (Rees and Alcolado 2005)

Kuo Kondo mouse (KK)

The KK mouse gradually becomes obese in adult life. Restriction of energy intake reduces both obesity and hyperglycemia seen in this mouse. Hypertrophy and degranulation of pancreatic islet-cells are observed in KK mice. The kidneys of these mice show typical changes of diabetic nephropathy such as diffuse and nodular glomerulosclerosis, and peripheral glomerular basement membrane thickening in addition to mesangial enlargement and hypercellularity. Proteinuria and microalbuminuria are also seen in this mouse strain. Therefore, the KK mouse serves as a good model for investigating obesity-associated diabetes mellitus in man (Ikeda 1994).

Nagoya–Shibata–Yasuda mouse (NSY)

NSY mice spontaneously develop diabetes in an age-dependent manner. Key features include impaired insulin secretion and mild insulin resistance. Obesity and extreme hyperinsulinemia are not commonly seen in these animals. Interestingly, almost all males develop hyperglycemia, but less than a third of females are affected. The NSY mouse is particularly useful when considering age-related phenotypes of

type 2 diabetes mellitus and for investigating the pathogenesis and genetic predisposition to the non-insulin dependant diabetes type (Ueda et al., 1995).

Otsuka Long-Evans Tokushima fatty rat (OLETF)

The OLETF rat can be traced back to an outbred colony of Long-Evans rats selectively bred for glucose intolerance. The characteristic features of OLETF rats are the late onset of hyperglycemia (after 18 weeks of age), the chronic course of the disease, the mild obesity, the clinical onset of diabetes mellitus mostly seen in males, and the hereditary trait. The changes of pancreatic islets proceed to a pathological stage showing, among others, atrophy of the islets. Diabetic nephropathy as seen in these rats, is demonstrated by diffuse glomerulosclerosis, and nodular lesions. These clinical and pathologic features of this illness in OLETF rats resemble those of human type 2 diabetes mellitus (Kawano et al., 1994).

Israeli sand rat (*Psammomys obesus*)

Originally, the Israeli sand rat feeds on a low-caloric-vegetarian diet. If, under laboratory conditions, fed a laboratory chow, the rats develop an obese diabetic syndrome with hyperinsulinemia, hyperglycemia, markedly decreased glucose tolerance, and insulin resistance, with its onset at thee months of age and forward. The hyperglycemic state is associated with an increase in circulating proinsulin and split products supposedly being caused by the high demand for insulin secretion due to insulin resistance, similar to human type 2 diabetes mellitus. Impaired insulin biosynthesis within the islets has also been reported. This rat model is particularly useful when investigating the effects of diet and exercise on the development of type 2 diabetes mellitus in humans (Marquie et al., 1984, Rees and Alcolado, 2005) .

Ob/ob mouse

The ob/ob mouse is a monogenic model of obesity, carrying a mutation in the leptin gene, the ligand for the leptin receptor, provoking leptin deficiency. Animal models of obesity have been used in an attempt to gain insights into the human condition. But since the mutation of leptin is a very rare cause of obesity and type 2 diabetes in humans, the ob/ob mouse serves only as a poor model for the research in human diabetes mellitus type 2 (Breyer et al., 2005).

Zucker diabetic fatty rat (ZDF; *fa/fa*)

The Zucker diabetic fatty rat, derived from inbreeding of hyperglycemic Zucker obese rats, is characterized by a mutation in the leptin receptor leading to high circulating leptin levels (Schmidt et al., 2003). The progression to diabetes mellitus in ZDF rats is due to a failure to increase beta cell mass in the pancreas, whereas human type 2 diabetes results from increased pancreatic islet amyloid formation. It is also reported that in the ZDF rat model of type 2 diabetes mellitus there is a significant incidence of hydronephrosis. Hydronephrosis is characterized by the dilation of the renal pelvis, compression of the papilla, and atrophy of the renal parenchyma; these features bear no relationship to diabetic nephropathy. This raises serious questions regarding the validity of the ZDF rat as a model for studying the renal consequence of diabetes mellitus in man (Marsh et al., 2009).

db/db mouse

The diabetic gene (*db*) is transmitted in an autosomal recessive manner. The *db* gene encodes for a point mutation of the leptin receptor, leading to abnormal splicing and defective signaling of the adipocyte-derived hormone leptin. Lack of leptin signaling in the hypothalamus will lead to persistent hyperphagia and obesity with consequently high leptin and insulin levels. Hyperinsulinemia in *db/db* mice is obvious at 10 days of age and blood glucose levels are slightly elevated at 1 month of age. After 5 to 6 months of age, the body weight and insulin levels begin to fall in association with pancreatic islet-cell degeneration, thus rapidly increasing hyperglycemia sets in as the remaining beta cells are unable to maintain the high levels of insulin secretion required. The *db*/*db* mouse also has a long history as a model of human diabetic nephropathy. Key common features with the human condition are renal hypertrophy, glomerular enlargement, albuminuria, and mesangial matrix expansion. Because this model appears to exhibit the most consistent and robust increase in albuminuria and mesangial matrix expansion, it has been used as a model of progressive diabetic renal disease (Sharma et al., 2003).

Fat-fed streptozotocin-treated rat (fat-fed/STZ rat)

The fat-fed/STZ rat originates from a non-obese, outbred rat strain of type 2 diabetes mellitus that replicates the prevalent background and metabolic characteristics of the human metabolic syndrome. Sprague-Dawley rats are fed a high-fat diet (40% of

calories as fat) for two weeks and then injected with low-dose streptozotocin. Fat-fed/STZ rats provide a feasible animal model for type 2 diabetes, simulating the human syndrome. This mouse model is suitable for the testing of anti-diabetic therapies (Reed et al., 2000).

CBA/Ca mouse

The CBA mouse was developed by crossing the Bagg albino with the DBA (Dilute Brown Non-Agouti) mouse. When brought to Great Britain by Carter, it was renamed CBA/Ca (Rithidech et al., 1999). Mature male CBA/Ca mice develop a spontaneous mild diabetes-obesity syndrome resembling human type 2 diabetes mellitus. This is characterized by hyperglycemia, hyperinsulinemia and insulin resistance. The pancreas of mature obese mice possesses significantly enlarged islets. Pancreatic beta cells do not degenerate and circulating insulin levels remain high throughout life. The mature male CBA/Ca mouse serves as a valuable model for investigating the etiology of type 2 diabetes mellitus (Figueroa and Taberner 1994).

Spontaneously Diabetic Torii (SDT) rat

Clinical characteristics of the SDT rats are hyperglycemia and hypoinsulinemia (from 25 weeks of age); long-term survival without insulin treatment, and hypertriglyceridemia (by 35 weeks of age). This rat model resembles human non-obese severe type 2 diabetes mellitus with insulin hyposecretion. The SDT rat is considered to be a potentially useful model for studies of diabetic retinopathy encountered in humans (Shinohara et al., 2000).

New Zealand obese (NZO) mouse

The NZO mouse has a polygenic syndrome that resembles human metabolic syndrome, with hyperphagia, obesity and insulin resistance, associated with hyperinsulinemia, hyperglycemia, hypercholesterolemia, and hyperleptinemia. This mouse model develops obesity and its related complications, leading to micro- and macrovascular injury, atherosclerosis, diabetes, hypertension and pathological angiogenesis (Balwierz et al., 2009).

Tsumura Suzuki Obese Diabetes (TSOD) mouse

The TSOD mouse is a relatively new polygenetic model of spontaneous type 2 diabetes mellitus, established as an inbred line in 1992 (Suzuki et al., 1999). Male TSOD mice show severe obesity, hyperglycemia, glucosuria, hyperinsulinemia, hyperlipidemia, including high density lipoprotein (HDL)-cholesterol, and abnormality of the pancreas and kidney. The TSOD mouse is a good model for studying diabetes-induced dysfunction of the kidney and pancreas (Kawada et al., 2010).

2.3.1.3 Animal models of diabetic kidney disease

Diabetic nephropathy in humans is a major complication of diabetes mellitus. It is a progressive disease that leads to end-stage renal failure, which requires renal replacement therapy such as dialysis or renal transplantation. Late stage diabetic nephropathy is characterized by severe glomerulosclerosis, reduced GFR, interstitial immune cell infiltrates, tubular atrophy, and interstitial fibrosis. In order to develop more effective therapies for these sequelae, the pathophysiological mechanisms of this illness need to be clarified in more detail. For this purpose, it is necessary to carry out medical science studies in animal models.

KK-A^y mouse

The KK- A^y mouse is a model of type 2 diabetes mellitus. It was produced by transferring the yellow obese gene (A^y allele) into the KK (Kuo Kondo) mouse. The diabetic nephropathy phenotypes in this mouse model are more severe than those in the original KK mouse. Also, the pathologic kidney findings in the KK- A^y mouse resemble those in humans, both immunohistochemically and pathologically. Histopathologic alterations in the kidneys of KK-A^y mice are, among others, gradual progression of glomerular damage with age, expansion of mesangial matrices, nodular lesions, and tubulointerstitial damage. (Yabuki et al., 2010).

Diabetic eNOS knockout mice

Nitric oxide (NO) is an endothelial cell-derived vasodilator which is an important modulator of permeability in the vasculature. In diabetes, the vascular endothelial NO synthase (eNOS) activity is altered and the functionally significant polymorphisms in the *NOS3* gene lead to lower production of NO. This is associated with the development of advanced nephropathy in patients with type 1 and type 2 diabetes.

Targeting of *Nos3*, the gene encoding eNOS, induces nephropathic changes in mouse models of both type 1 (streptozotocin induced) and type 2 (db/db mouse) diabetes that mimic many aspects of human disease. Systemic depletion of eNOS on a diabetic background allows the study of both vascular and renal pathology in the same animal. Moreover, eNOS knockout mice on a db/db background can readily be used to evaluate the efficacy of drug therapy to target multiple-organ pathologies (Mohan et al., 2008). A model of type 1 diabetes with deficient eNOS activity was produced by inducing diabetes by low-dosage streptozotocin (STZ) injection in *eNOS* deficient mice. These diabetic *eNOS* mice develop significant increases in mesangial expansion, mesangiolysis, and focal sclerosis. Type 2 diabetic eNOS deficient db/db mice develop significant albuminuria, decreased glomerular filtration rate, mesangial expansion, glomerular basement membrane thickening, arteriolar hyalinosis, mesangiolysis, nodular glomerulosclerosis, and tubulointerstitial injury that is significantly greater than that found in the low-dosage STZ diabetic eNOS knockout mice (Brosius et al., 2009).

Bradykinin B2 Receptor (B2R) deficient *Ins2*$^{Akita/+}$ mouse

The targeted deletion of the bradykinin 2 receptor contributed to the evolution of diabetic nephropathy in *Ins2*$^{Akita/+}$ mice on a B6 background. This mouse model showed a four-fold increase in albuminuria and profound mesangial expansion that resembles the glomerular changes seen in human diabetic glomerulosclerosis. There are no changes in the glomerular endothelial cells or podocytes. The mice also develop mitochondrial DNA damage in the kidneys and other tissues, indicating generalized aging (Kakoki et al., 2004). In contrast, Akita mice with functional B1 and/ or B2 receptors are not considered a robust model of nephropathy (Brosius et al., 2009).

Decorin deficient streptozotocin diabetic mouse

Decorin is a small, leucine-rich proteoglycan that is primarily secreted and stored in the extracellular matrix. Decorin can inhibit transforming growth factor beta (TGF-ß) activation by binding to the active form of TGF-ß. TGF-ß is a profibrotic cytokine involved in the pathogenesis of diabetic renal disease. Decorin is constantly stimulated in diabetic nephropathy. The decorin null mouse on a B6 background develops enhanced features of nephropathy. Decorin deficiency substantially

worsens the progression of diabetic kidney disease in streptozotocin diabetic mice, with features that closely mimic advanced human diabetic nephropathy. Diabetic mice with decorin deficiency have increased albuminuria, impaired renal function, and an increased degree of mesangial matrix expansion with fibrin caps and macrophage infiltration. These results conclusively identify decorin as a protective agent in this murine model of diabetic nephropathy (Williams et al., 2007).

NONcNZO mouse

The NONcNZO mouse model is an inbred congenic strain derived from a cross between the Nonobese Nondiabetic (NON) mouse and the New Zealand Obese (NZO) mouse, which provides a model of polygenic type 2 diabetes. Unlike mice with null mutations in a single gene producing morbid obesity, this mouse model develops milder obesity produced by the interaction of numerous genes with relatively small effects (Leiter and Reifsnyder 2004). After approximately 8 months of age, NONcNZO mice develop significant and progressively increasing albuminuria. Glomerular histopathology is impressively abnormal but, in addition to glomerulosclerosis, exhibits features that are atypical for diabetic nephropathy (Brosius et al., 2009).

OVE26 mouse

The OVE26 mouse (overexpression) is a transgenic model of early-onset type 1 diabetes. These mice develop diabetes within the first weeks of life as a result of beta cell toxicity in response to overexpression of the calmodulin gene under the control of the insulin promoter. However, a low level of beta cell survival allows OVE26 heterozygotes to live and maintain their body weight well over 1 year with no insulin treatment. Progressively increasing albuminuria occurs at 9 months of age in conjunction with hypalbuminemia, high blood pressure, and decreasing GFR. These mice develop progressively enlarged glomeruli, with diffuse and nodular expansion of mesangial matrix, tubulointerstitial fibrosis, and thickening of the glomerular basement membrane. This model is useful for better understanding and treatment of diabetic nephropathy (Zheng et al., 2004).

Black and tan, brachyuric (BTBR) *ob/ob* mouse

BTBR *ob/ob* mice develop a variety of abnormalities that closely resemble advanced human diabetic nephropathy more rapidly than most other murine models. The BTBR mouse strain with the *ob/ob* leptin-deficiency mutation develops severe type 2 diabetes, hypercholesterolemia, elevated triglycerides, and insulin resistance. These obese, diabetic mice briskly reveal morphologic renal lesions characteristic of both early and advanced human diabetic nephropathy. Also a persisting, early onset loss of podocytes is present. The BTBR ob/ob mouse strain is suggested to be particularly interesting for testing therapeutic interventions for diabetic kidney disease (Hudkins et al., 2010).

2.3.2 GIPR^{dn} transgenic mice

This transgenic diabetic mouse model expresses a dominant negative GIP (glucose-dependent insulinotropic polypeptide) receptor (GIPR^{dn}) in pancreatic beta cells, leading to the development of severe early onset diabetes mellitus. GIP is an incretin hormone, which is released after food intake from the small intestine. GIP produces multiple physiological effects, including increase in glucose-mediated insulin secretion, insulin gene transcription, and may act as a mitotic and anti-apoptotic agent in pancreatic beta cells. In order to illustrate the role of the GIP receptor within the enteroinsular axis *in vivo*, the expression of a dominant negative mutant of the GIPR in transgenic mice was implemented. The cDNA of the human GIPR was mutated at the third intracellular loop by a deletion of eight amino acids (positions 319 to 326) and a point mutation a position 340. The malfunction of this mutated GIPR was demonstrated *in vitro*. Transgenic mice were then generated, expressing the mutated human GIPR cDNA under the control of the rat pro-insulin 2 gene promoter in pancreatic beta cells. These GIPR^{dn} transgenic mice show an early disturbance in pancreatic islet development seen in highly reduced beta-cell mass, disturbed composition of islets, and decreased islet neogenesis (Herbach et al., 2005). Furthermore, decreased insulin secretion and early onset diabetes mellitus, without obesity or insulin resistance are evident (Herbach et al., 2008). GIPR^{dn} transgenic mice display glucosuria between 14 and 21 days of age. By the age of 30 days, the blood glucose levels of transgenic mice are largely elevated and an absolute insulin deficiency is observed (Herbach et al., 2005). Development, dimensions and histological patterns of kidney lesions detected in GIPR^{dn} transgenic

mice show similarities to diabetes-associated kidney injury of humans, consequently making $GIPR^{dn}$ transgenic mice a promising animal model for studying the onset and progression of diabetic nephropathy (Herbach et al., 2009).

2.3.3 Remnant kidney animal models

It remains difficult to address the progression of kidney lesions in animal models, since advanced diabetic nephropathy develops over more than a decade in humans. As a matter of fact, all commonly used rodent models of diabetic nephropathy don't display significant tubulointerstitial lesions during a period of 6 months. Experimental means that intend to accelerate the development of end-stage kidney disease in mice should enhance crucial pathomechanisms of diabetic nephropathy (Ninichuk et al., 2007). In scientific animal studies, chronic renal failure is mostly achieved by partial removal of renal parenchyma. The two most common techniques used are infarction and subtotal nephrectomy (remnant kidney model). The remnant kidney model may be achieved by either ligation of renal vessels supplying the renal poles or surgical excision of both renal poles followed by contralateral nephrectomy (Liu et al., 2003).

Since the first publication of a remnant kidney model in 1889, numerous investigators studied kidney disease by surgically reducing the kidney mass by ½, ⅔ or ¾ in various animal species. In 1932 the $^5/_6$ nephrectomy (5/6Nx) rat model which has been used ever since was developed (Chanutin and Ferris 1932). Another way of producing experimental renal failure is the administration of nephrotoxic agents. Nephrotoxic drugs exert a lot of undesirable side-effects including cardiotoxicity (Sviglerova et al., 2010).

5/6 surgical nephrectomy in rats

In Wistar male rats chronic renal failure is induced by 5/6 surgical nephrectomy. This is achieved by unilateral nephrectomy plus either surgical ablation of 2/3 of the other kidney or selective ligation of extrarenal branches of the left renal artery such that approximately 2/3 of the left kidney is infarcted. This model closely resembles chronic renal failure in humans, including cardiovascular complications, it shows a high degree of reproducibility and a minimum of undesirable side-effects. Thus, the present rat model of subtotal surgical renal mass reduction represents a useful tool in

the study of chronic renal failure and its cardiovascular complications (Sviglerova et al., 2010).

3/4 surgical nephrectomy in rabbits

The rabbits underwent bipolar left nephrectomy and complete removal of the right kidney. Four weeks after nephrectomy, a loss of 75% of the left renal mass is confirmed. The animals developed chronic renal failure, and an increase in size of the left kidney remnant can be seen at 16 weeks of age. Histological evaluation showed subcapsular and interstitial fibrosis and also tubular regeneration. This model of chronic renal failure was suggested to be valuable for testing different approaches to repair kidney damage (Costa et al., 2009).

Uninephrectomy in db/db mice

At 24 weeks of age, uninephrectomized db/db mice reveal increased albuminuria and severe glomerulosclerosis in 37% of glomeruli as compared to sham-operated controls. Uninephrectomy also increases the number of glomerular macrophages in db/db mice. The uninephrectomy-related acceleration of glomerular damage is associated with significant tubulointerstitial injury as indicated by an increase in indices of tubular cell damage, tubular dilatation, and expansion of interstitial volume. Uninephrectomy may be a preferred method of accelerating diabetic nephropathy in db/db mice because it does not affect unrelated or other pathomechanisms of this disease (Ninichuk et al., 2007).

Uninephrectomy in mice treated with VEGF

Vascular endothelial growth factor (VEGF) is essential for normal renal development and plays a role in diabetic glomerular enlargement. Unilateral nephrectomized mice treated with VEGF-Antibody show suppressed glomerular enlargement and partially blocked renal growth without affecting body weight or food consumption. Uninephrectomized mice that did not receive VEGF-Antibody display an increase in glomerular volume and kidney weight. These findings indicate that VEGF plays a major role in the glomerular compensatory response after uninephrectomy (Flyvbjerg et al., 2002).

3. Research design and methods

3.1 Animals

All animal experiments were performed in accordance with institutionally approved and recent animal care guidelines underlying the German animal welfare bill (BGBI I p. 1105), AZ 55.2-1-54-2531-100-06.

Mice investigated in this study were exclusively male heterozygous transgenic mice that express a dominant-negative glucose dependent insulinotropic polypeptide receptor ($GIPR^{dn}$) and age-matched non-transgenic littermate controls. The animals received a standard breeding diet (Altromin 1324, Germany) and tap water ad libitum. They were maintained on a 12 h- light and 12 h- darkness cycle. Mice were weaned at 3 weeks p.p., separated according to gender, marked by piercing of the ears, and tail tip biopsies for genotype analyses were taken. The chosen male animals undertook surgery, i.e. uninephrectomy or sham operation, at 1 month of age. In the course of this study, urine samples of each mouse were taken in monthly intervals and body weights were recorded biweekly. Animals were euthanized at 6 or 12 months of age.

3.1.1. Genotyping

Transgenic mice were identified by polymerase chain reaction as described as follows, using DNA extracted from tail tips, according to standard protocols (Herbach et al., 2005, Hoeflich et al., 2001).

3.1.1.1 Primers

For the identification of $GIPR^{dn}$ transgenic mice, oligonucleotide primers with the following sequence were used:

-5'- ACA GNN TCT NAG GGG CAG ACG NCG GG-3' sense (Tra1)

-5'- CCA GCA GNC NTA CAT ATC GAA GG-3' antisense (Tra3)

(Synthese, LMU, Munich, Germany)

These primers bind to the human cDNA of the mutated GIP receptor and also to the endogenous murine GIP receptor. The primers were chosen from areas where the known DNA sequence of the human, rat, mouse and hamster GIP receptor is highly

conserved. Wherever the sequence varies in these animals, oligonucleotide synthesis was performed to allow all nucleotides ("N" in primer sequence) to integrate (Herbach et al., 2005, Volz, 1997). The mutated human GIP receptor and the endogenous murine receptor can be distinguished in the PCR by their number of base pairs. The PCR product of the murine GIP receptor contains about 500 base pairs, whereas the PCR-product of the mutated human GIP receptors consists of about 140 base pairs.

3.1.1.2 DNA isolation

At weaning of mice, tail tip biopsies were taken and stored at -20°C until assayed. For DNA extraction, a tail tip of approximately 0.5 cm length was incubated in 400 µl Mastermix over night in a heating block (Biometra TB1 Thermoblock, Whatman, Germany) at 55°C. Thereafter, undigested components were separated by centrifugation for two minutes at 15,000 rpm (Sigma 1K15, Sigma, Germany). The supernatant was poured into another tube (Eppendorf safe lock tube, Eppendorf AG, Germany) and 400 µl isopropanol (Roth, Germany) were added to precipitate DNA. The DNA pellet was washed twice with 900 µl 70% ethanol (Roth, Germany), the liquid phase was discarded and the DNA pellet was dried at room temperature. DNA was suspended in 100 – 200 µl 1xTE buffer, according to the size of the pellet when dried. To make sure that the DNA was dissolved completely it was stored at 4°C for at least 24 hours before proceeding with the PCR.

Mastermix

Cutting buffer	375 µl
SDS 20% (Sodiumdodecylsulfate Ultra Pure, Roth, Germany)	20 µl
Proteinase K (20mg/ml) (Boehringer Ingelheim, Germany)	5 µl

Proteinase K

20 mg/ml were dissolved in aqua bidest., aliquoted and stored at –20°C.

Cutting buffer

1 M Tris-HCl (pH 7.5, Roth, Germany)	2.5 ml
0.5 M EDTA (pH 8.0, Sigma, Germany)	5.0 ml
5 M NaCl (Roth, Germany)	1.0 ml
1 M DTT (Roth, Germany)	250 µl

Spermidine (500mg/ml, Sigma, Germany)	127 µl
Aqua bidest	ad 50 ml

Storage at 4°C

TE-buffer
10 mM Tris-HCl (pH 8.0, Roth, Germany)
1 mM EDTA
Storage at 4°C.

3.1.1.3 Polymerase chain reaction (PCR)

One µl of the suspended DNA was mixed with 19µl of the Master Mix in PCR-analysis cups (Kisker, Germany). DNA and components of the Mastermix were kept on ice during the procedure. The Taq DNA polymerase was stored at -20°C until it was added to the Mastermix. Taq DNA polymerase and Mastermix reagents were from the Taq PCR Master Mix Kit (Qiagen, Germany).

Until further use, the PCR samples were stored at either 4°C (short-term) or at -20°C (long-term). DNA of a transgenic mouse was used as positive control, DNA of a wild-type mouse was used as negative control and H_2O served as quality (no template) control. The PCR was run in a Biometra® Uno II Thermocycler (Biometra, Germany), programmed as described:

Mastermix			**PCR-conditions**			
Aqua bidest.		3.65 µl	denaturation	94 °C	4 min	
Q-solution		4.00 ul	denaturation	94 °C	1 min	
10 x buffer		2.00 µl	annealing	60 °C	1 min	39 x
MgCl2		1.25 µl	extension	72 °C	2 min	
dNTP's (1mM)		4.00 µl	final extension	72 °C	10 min	
sense primer	(Tra 1: 10 pM)	2.00 µl				
antisense primer	(Tra 3: 10 pM)	2.00 µl				
Taq Polymerase		0.10 µl				
template		1.00 µl				

3.1.1.4 Gel electrophoresis

DNA fragments were separated by size via electrophoresis in a TAE agarose (1.5%) gel (1.5 g agarose (Gibco BRL, Germany)/100 ml 1xTAE buffer), containing 9 µl/l ethidiumbromide (0.1%, Merck, Germany), casted in a Easy Cast® gel chamber (PeqLab, Germany) and filled with 1x TAE running buffer. The TAE running buffer also contained 9 µl/l ethidiumbromide (0.1%). Ethidiumbromide binds to double stranded DNA by interpolation between the base pairs and fluorescence may be seen when irradiated in the UV part of the spectrum. DNA samples were colored with 4 µl of 6x loading dye (MBI Fermentas, Germany). At the beginning of each sample well row, 12 µl PUC Mix Marker #8 (MBI Fermentas, Germany) were placed in order to allow estimation of amplified fragment size. The remaining wells were filled with 24 µl of the samples.

Then electrophoresis was run for approximately 45 minutes at 90 V with an output of approximately 200 mA (Biorad Power PAC 300, Biorad, USA). Subsequently, the amplified products were visualized (Eagle Eye II, Stratagene, Germany) under UV light (306 nm) and a digital picture was taken to document the result.

50x TAE stock solution

Tris base (Roth, Germany)	121 g
glacial acetic acid (Sigma, Germany)	28.55 ml
EDTA, 0.5 M, pH 8.0 (Sigma, Germany)	50 ml
ad 500 ml distilled water	

1x TAE-buffer

10 ml 50x TAE-buffer ad 500 ml distilled water

3.1.2 Uninephrectomy

Initially, all mice were weighed to determine the correct dose of anesthesia.

Urine was collected from each animal and 10 µl Meloxicam (Metacam®, 1.5 mg/ml, Boehringer, Germany) was administered orally.

Mice were anesthetized by intraperitoneal injection of medetomidin (Domitor®, 1 mg/ml, Pfizer AG, Germany), midazolam (Dormicum®, 5 mg/ml, Roche Pharma, Germany) and fentanyl (Fentanyl®- Janssen, 0.05 mg/ml, Janssen-Cilag, Germany).

After the anesthetic injection the mice were kept under an infrared heating lamp to stabilize the body temperature.

As soon as surgical tolerance was reached, the mouse was placed on a warming-pad. Eye ointment (Bepanthen®, Bayer, and Germany) was applied to both eyes and the coat was shaved from shoulder to hip on the left side. Following disinfection of the skin, an incision of approximately 1 cm was made vertically behind the costal arch. The left kidney was advanced, decapsulated and retained at the renal hilus by forceps. Below the forceps a ligature was made and the kidney was removed. The muscular layer was sutured with absorbable suture material (Vicryl, ETHICON, Germany). The skin was occluded with surgical clamps and wound powder (Sulfonamid-Kombi-Puder, Albrecht, Germany) was applied.

The anesthesia was antagonized by intraperitoneal injection of atipamezol (Antisedan®, 5 mg/ml, Pfizer AG, Germany), flumazenil (Anexate®, 0.1 mg/ml, Roche Pharma, Germany) and naloxon (Narcanti®, 0.4 mg/ml, Bristol-Myers Squibb GmbH, Germany). The mice were placed under an infrared heating lamp until fully awake.

In the following 5 days, each mouse was clinically examined and 10 µl Meloxicam (Metacam®, 1.5 mg/ml, Boehringer, Germany) was administered orally.

10 days after the surgery, the surgical clamps were removed and normal hair growth was observed.

3.2 Body weights

Starting with the day of surgery at about 1 month, all animals were weight in intervals of 14 days. Last documentation of body weight was shortly before euthanasia. Body weight was determined to the nearest 0.1 g, using a precision scale (Kern KB 5000-1, Kern & Sohn GmbH, Germany).

3.3. Blood pressure

Blood pressure was non-invasively measured at 2 and 9 months of age by determining the tail blood volume with a volume pressure recording sensor and an occlusion tail-cuff (CODA System, Kent Scientific, USA).

3.4 Blood glucose

Blood glucose levels were measured in all mice at weaning. Blood was collected from the tail vein by drawing 10 µl blood into a capillary. The blood samples were immediately put into an Eppendorf cup containing 500 µl hemolysing solution (Roche, Germany). The blood glucose levels were determined using the Super GL_{easy} (Hitado, Germany). The system was calibrated with a control solution of known concentration and then the samples were measured.

3.5 Serum parameters

Blood was collected from the tail vein prior to euthanasia at 6 and 12 months and before 24 hour urine collection at 4 months of age. Serum was separated by centrifugation (10 min, 10,000 x g) and stored at -80°C until assayed.
All serum samples were screened for chloride, total protein, creatinine, urea, triglyceride, glucose and albumin. Screening was performed with the Architect ci8200 Autoanalyser (Abbott, Germany) and reagents supplied by Abbott. The testing was kindly done at the City Clinic Munich in Schwabing, Germany.

3.6 Urine protein analysis

Urine protein analysis was performed in order to evaluate clinical features of kidney damage. Urine samples were collected in monthly intervals between 1 and 6 months of age. Urine samples were always taken between two and three o'clock in the afternoon and immediately stored at -80 °C until assayed. In addition, the 24 hour urine was collected using metabolic cages (Techniplast, Germany) at the age of four months in all animals.

3.6.1 Sodium dodecyl sulfate (SDS) polyacrylamide gel electrophoresis (PAGE)

At first, urine creatinine concentration was measured (kindly performed at the Medizinische Kleintierklinik, LMU Munich) using an automated analyzer technique (Hitachi, Merck, Germany). Urine samples were then diluted to a creatinine content of 1.5 mg/dl, but at least 1:2 with reducing sample buffer. Subsequently, the diluted

samples were heated in a thermoblock TB1 (Biometra, Germany) for 10 minutes at 100°C for denaturation of the proteins. In the meantime, a SDS-12% polyacrylamide gel was casted in a gel-casting chamber (Mini-Protean III, Biorad, Germany) and covered with isopropanol. After polymerization, the stacking gel was casted onto the SDS-12% gel; a comb for forming sample wells was immediately placed in the still fluid stacking gel. When the stacking gel was fully polymerized, the comb was removed and the gel was placed into an electrophoresis cell (Protean III, Biorad, Germany) which was then filled with running buffer to the top of the inside cell. The samples, a broad molecular weight standard (Biorad, Germany) and a mouse albumin standard (Biotrend, Germany) diluted 1:100 in sample buffer were then loaded onto the gel and electrophoresis was run for 60 minutes at 200 volt. The gel was removed from the glass frame and silver staining was performed due to a standard protocol (see 9.1). Clearly visible gel bands were registered and gels were photographed for documentation. Finally, gels were dried according to the manufacturer's protocol (see 9.2), using the DryEase™Mini-Gel Drying System (Novex, Germany) for long-term storage. Materials used are listed below.

Sample buffer
- 1 ml Distilled water
- 0.25 ml Tris/HCl (Roth, Germany) 0.5 M pH 6.8
- 0.2 ml Glycerol (Merck, Germany)
- 0.4 ml SDS (Sigma, Germany) 10%
- 0.125 ml Bromphenol blue (Sigma, Germany) 0.05%

Tris/HCl 0.5 M pH 6.8
- 6.075 g Tris base (Roth, Germany)
  ad 60 ml distilled water, adjust pH using 1N HCl (Merck, Germany)

Running buffer (stock)
- 30.3 g Tris base (Roth, Germany)
- 144 g Glycine (Merck, Germany)
  ad 1 l distilled water

Running buffer (ready to use)
- 40 ml Stock solution
- 4 ml SDS (Sigma, Germany), 10%
  ad 400 ml distilled water

SDS-12% polyacrylamide gel
- 3.5 ml Distilled water
- 2.5 ml Tris/HCl (Roth, Germany) 1.5 M, pH 8.8
- 100 µl SDS (Sigma, Germany) 10%
- 4.0 ml Acrylamide (Roti Phenol, Germany)

50 µl Ammonium persulfate 10% (Biorad, Germany)
5 µl Tetraethylethylenediamine/ TEMED (Sigma, Germany)

Stacking gel
6.1 ml Distilled water
2.5 ml Tris/HCl (Roth, Germay) 0.5 M, pH 6.8
100 µl SDS (Sigma, Germany) 10%
1.3 ml Acrylamide (Roti Phenol, Germany)
50 µl Ammonium persulfate 10% (Biorad, Germany)
5 µl Tetraethylethylenediamine/ TEMED (Sigma, Germany)

3.6.2 Mouse albumin enzyme linked immuno-sorbent assay (ELISA)

In addition to qualitative determination of proteinuria by SDS-PAGE, urinary albumin excretion was quantified by ELISA, using the mouse albumin ELISA-kit Bethyl E90-134 (Bethyl, USA), according to the manufacturer's protocol. All steps were performed at room temperature. Coating and blocking of plates was performed according to the manufacturer's recommendations: 1 µl (1 mg/ml) of goat anti-mouse albumin capture antibody (A90-134A) was diluted to 100 µl coating buffer for each well to be coated. The coated plate (Nunc C bottom Immunoplate 96 well, Nunc A/S, Denmark) was incubated for 60 minutes. After incubation, the capture antibody solution was aspirated from each well. Each well was then filled with wash solution, which then was removed by aspiration. These washing steps were repeated for a total of 3 washes. 200 µl of blocking (post-coat) solution were then added to each well and the plate was incubated for 30 minutes. After incubation, the blocking (post-coat) solution was removed and each well was washed three times as described above. The murine albumin standard (calibrator) dilutions were prepared due to manufacturer's recommendations (range: 7.8 - 500 ng/ml). Standards were diluted in sample diluent as described in table 2 below. The urine samples were diluted with sample diluent, based on the expected concentration of the analyses to fall within the concentration range of the standards. The proper dilution of urine specimens ranged from 1:50 - 1:1,600 ($GIPR^{dn}$ tg: 1:50 - 1:1,600, associated controls: 1:300 - 1:600), as shown by a pilot study. Standards, samples, blanks and controls were analyzed in duplicates. Each 100 µl of standards or samples were transferred to the assigned wells. The plate was then incubated for 60 minutes. After incubation, samples and standards were removed and each well was washed 5 times as described above. The HRP conjugate (goat anti-mouse albumin-HRP conjugate, 1 mg/ml) was diluted

in conjugate diluent 1:100,000. 100 µl of diluted HRP conjugate were transferred to each well and the plate was then incubated for 60 minutes. After incubation, the free HRP conjugate was removed and each well was washed 5 times. Subsequently, bound HRP antibody conjugate was detected through a chromogenic reaction. The substrate solution (TMB/H_2O_2, Kirkegaard and Perry, USA) was prepared by mixing equal volumes of the two substrate reagents, provided by the manufacturer. 100 µl of substrate solution were added to each well and incubated for seven minutes. The TMB reaction was stopped by adding 100 µl of 1 M H_3PO_4 (Roth, Germany) to each well. The color intensity was measured by determining the absorbance at 450 nm using a computer-assisted (Magellan, Tecan AG, Germany) microplate reader (Sunrise, Tecan AG, Germany). For calculation of results, the duplicate readings from each standard, control and sample were averaged. The zero reading was subtracted from each averaged value above. A standard curve was generated for each set of samples (Magellan, Tecan AG, Germany). The values of the specimen wells were in the linear segment of the calibration curve. For each group and stage of investigation, the albumin/creatinine ratios were calculated by dividing the measured albumin concentration of a urine sample by its corresponding creatinine concentration. Materials used for performance of ELISA-analyses are indicated below.

Coating buffer

0.05 M Carbonate-bicarbonate (Sigma, Germany)
adjust to pH 9.6

Wash solution

50 mM Tris (Roth, Germany)
0.14 M NaCl (AppliChem, Germany)
0.05% Tween 20 (Roth, Germany)
adjust to pH 8.0

Blocking (postcoat) solution

50 mM Tris (Roth, Germany)
0.14 M NaCl (AppliChem, Germany)
1% Bovine serum albumin in Tris buffered saline (Sigma Chemical, Germany)
adjust to pH 8.0

Sample/conjugate diluent

50 mM Tris (Roth, Germany)

0.14 M NaCl (AppliChem, Germany)

1% Bovine serum albumin in Tris buffered saline (Sigma Chemical, Germany)

0.05% Tween 20 (Roth, Germany)

adjust to pH 8.0

step	ng/ml	calibrator	sample diluent
0	10000	2 µl	9 ml
1	500	0.5 ml from step 0	9.5 ml
2	250	1 ml from step 1	1 ml
3	125	1 ml from step 2	1 ml
4	62.5	1 ml from step 3	1 ml
5	31.25	1 ml from step 4	1 ml
6	15.625	1 ml from step 5	1 ml
7	7.81	1 ml from step 6	1 ml

Table 3: Preparation of murine albumin standard dilutions (range: 7.8 - 500 ng/ml) for quantification of urine albumin concentrations by ELISA (mouse albumin ELISA-kit Bethyl E90-134, Bethyl, USA)

3.7. Glomerular filtration rate

The glomerular filtration rate was calculated from serum creatinine, urine creatinine and 24 hour urine volume of samples collected in metabolic cages at 4 months of age as follows:

$$\text{creatinine}_{(\text{urine})} * \text{urine volume} / \text{creatinine}_{(\text{serum})}$$

3.8 Kidney preparation and morphometric analysis

At 1 month of age, the surgically removed left kidney was carefully separated from adjacent tissues, decapsulated, and weighed to the nearest mg, using a BP 61S scale (Satorius, Germany). The kidneys of 1-month-old animals were fixed by immersion in 4% neutral buffered formaldehyde solution, and processed for GMA/MMA- and Epon-embedding as described below.

3.8.1. Kidney perfusion

Kidneys of uninephrectomized and sham operated transgenic and control animals were fixed via orthograde vascular perfusion at 6 an 12 months of age. All mice were weighed prior to sacrifice. Mice were euthanised by intraperitoneal injection of 300 µl of ketamine/xylazine solution, containing 1 ml Ketamine 10% (Selectavet, Germany), 0.25 ml Xylazine 2% (Rompun 2%, Bayer, Germany), and 5 ml NaCl 0.9%.

Perfusion was performed by initially opening the abdominal and thoracic cavity via incision. The left ventricle was penetrated with the perfusion needle and on starting of the perfusate flow, the inferior vena cava was cut cranial of the diaphragm to provide outflow of the perfusate. First, the vasculature was pre-flushed with 2 ml Lidocain (Lidocainhydrochlorid 2%, bela-pharm, Germany) in order to dilate the blood vessels, followed by perfusion with about 40 - 50 ml PBS (pH 7.4, 37°C) to wash the blood out of the circulation. A slice of approximately 1 mm thickness was carefully cut from one pole of the right kidney, using a scalpel blade and frozen in liquid nitrogen. Then, perfusion with warm (37°C) 3% glutaraldehyde (6 month of age) or 4% paraformaldehyde (12 months of age) in PBS (pH 7.4) was performed for 5 minutes.

After postfixation for 24 hours in the same fixans used for perfusion, kidneys were removed carefully, separated from adjacent tissues, weighed to the nearest mg, cut perpendicular to the longitudinal axis into slices of approximately 2 mm thickness and samples for Epon embedding were taken by systematic random sampling (see below). In order to avoid distortions, the kidney slices were fixed with a piece of foam-rubber sponge (Bio Optica, Italy) in the tissue-embedding capsules (Engelbrecht, Germany). Embedding in glycolmethacrylate and methylmethacrylate (GMA/MMA) was performed (Hermanns et al., 1981). Kidney slices were immersed in a hydroxymethylmethacrylate (Fluka Chemie, Germany) / methylmethacrylate (Riedel de Haën, Germany) solution at 4°C on a shaker for 18 hours. The kidney slices were then shifted into “solution A”, composed of benzoylperoxide (338 mg; Merck, Germany), methylmethacrylate (20 ml), hydroxymethylmethacrylate (60 ml), ethyleneglycol monobutylether (16 ml; Merck, Germany) and polyethylene glycol 400 (2 ml; Merck, Germany). After immersion at 4°C on a shaker for four hours, the kidney slices were placed in plastic cups and embedded using 60 µl of dimethylanilin (Merck, Germany) in 40 ml of “solution 1” as starter for polymerisation. Embedding cups were immediately placed into a water bath (4°C) and polymerisation took place at 4°C over night. Sections of approximately 1.5 µm thickness were cut using a

Microm HM 360 rotary microtome (Microm, Germany), dried on a heating plate (OTS 40, Meditel, Germany) and stored in an incubator (Memmert, Germany) at 64°C over night before staining. Sections were stained with PAS (Periodic Acid Schiff stain), PASM (periodic acid silver methenamine) PAS, and H&E (Hematoxilin & Eosin), as indicated below.

3.8.2. Processing for plastic histology

Phosphate-buffered saline (PBS)

potassium dihydrogen phosphate (AppliChem, Germany) 0.25 g
sodium chloride (AppliChem, Germany) 8.0 g
di-sodium hydrogen phosphate dihydrate (AppliChem,Germany) 1.46 g
ad 1 l distilled water, adjust to pH 7.4

Dehydration

Rinsing solution	3 hours
Ethyl alcohol 30 %	2 x 1 hour
(Bundesmonopolverwaltung für Branntwein, Germany)	
Ethyl alcohol 56 %	2 x 1 hour
Ethyl alcohol 70 %	2 x 1 hour
Ethyl alcohol 96 %	2 hours
Ethyl alcohol 96 %	2 x 3 hours

Periodic acid-Schiff stain (PAS)

1. 1% periodic acid (Applichem, Germany)	15 minutes
2. Distilled water	3 times 3 seconds
3. Schiff‘s reagent (Merck, Germany)	30-60 minutes
4. Rinse in tap water	30 minutes
Dry	
Mayer‘s hemalaun (Applichem, Germany)	35 minutes
Rinse in tap water	10 minutes
1% HCl alcohol	1 second
Rinse in tap water	10 minutes
Dry	

Mount under glass cover slips using Histofluid® (Superior, Germany)

H&E staining

1. Mayer‘s hemalaun (Applichem, Germany)	30 minutes
2. Rinse in tap water	10 minutes
3. 1% HCl-Alcohol	1 second
4. Rinse in tap water	10 minutes
6. Dry	
7. Eosine Y (Merck, Germany)	5 minutes
8. Distilled water	3 times 3 seconds
9. Dry	
10. Mount with glass cover slips using Histofluid® (Superior, Germany)	

PASM PAS stain (Gomori 1946) modified

1.	1% periodic acid (Applichem, Germany)	15 minutes
2.	Distilled water	3 times 3 seconds
Dry		
Silver-methenamine solution containing:		
	3% Methenamine solution	50 ml
	5% Silver nitrate (Applichem, Germany)	2.5 ml
	2% Sodium tetraborate decahydrate (Borax)	6 ml
	Distilled water	45 ml
	Pre-heat to 60° in a water bath	5 minutes
Staining	(shake in a closed water bath at 60°C)	15-50 minutes, staining intensity has to be controlled repeatedly
Distilled water		3 times 3 seconds
1.5% Sodium thiosulphate solution		2 minutes
Rinse in tap water		5 minutes
Dry		
Schiff‘s reagent (Merck, Germany)		60 minutes
Rinse in tap water		30 minutes
Dry		
Mayer‘s hemalaun (Applichem, Germany)		25 minutes
Rinse in tap water		10 minutes
1% HCl alcohol		1 second

Rinse in tap water	10 minutes

Dry

Mount under glass cover slips using Histofluid® (Superior, Germany)

3.8.3. Tissue preparation for Epon embedding

For the preparation of semithin sections for quantitative stereological analyses in 1- and 6-month-old animals, three cubes (1mm^3) of cortical kidney tissue from each animal and kidney were taken by systematic random sampling, postfixed in 1% osmiumtetroxide (OsO_4, Merck, Germany), dehydrated and embedded in Epon (syn. “glycid ether 100”, Serva, Germany) according to standard procedures: The samples were washed for 3 hours in Sörensen phosphate buffer at room temperature, postfixed in 1% osmium tetroxide (Caulfield 1957) for 2 hours at 4°C, and washed in Sörensen phosphate buffer three times for 2 min at room temperature. Subsequently, the specimens were dehydrated through a series of acetone (Roth, Germany) solutions at 4°C. Then they were infiltrated with a 100% acetone/Epon mixture for 1 hour, and twice with pure Epon for 30 min each, at room temperature. Then, the Epon infiltrated samples were embedded in Epon-embedding mixture in dried gelatin capsules (Plano, Germany). Polymerization took place at 60°C for approximately 48 hours. Epon blocks were trimmed with a TM60 Reichert-Jung milling machine (Leica, Germany) and 0.5 µm semi-thin sections were obtained with a Reichert-Jung "Ultracut E" (Leica, Germany). Sections were then stained with Azur II/Safranin, as indicated below.

The following materials were used for Epon histology:

Sörensen phosphate buffer 0.067 M, pH 7.4

Solution I	80.8 ml
Solution II	19.2 ml

adjust to pH 7.4

Solution I

potassium dihydrogen phosphate (Roth, Germany)	9.08 g

ad 1 l distilled water

Solution II

di-sodium hydrogen phosphate dihydrate (Roth, Germany)	11.88 g

ad 1 l distilled water

Veronal acetate buffer, pH 7.6

sodium veronal (barbitone sodium, Merck, Germany)	2.95 g
sodium acetate (Merck, Germany)	1.94 g
ad 100 ml distilled water	

Osmium tetroxide, 1%

osmium tetroxide, 2% (Merck, Germany)	5.0 ml
veronal acetate buffer, pH 7.6	2.0 ml
hydrogen chloride 0.1 M (Merck, Germany)	2.0 ml
distilled water	1.0 ml
Saccharose (Merck, Germany)	0.45 g

Solution A

glycid ether 100 (Serva, Germany)	62 ml
2-dodecenyl succinicacid anhydride (Serva, Germany)	100 ml

Solution B

glycid ether 100 (Serva, Germany)	100 ml
methylnadic anhydride (Serva, Germany)	89 ml

Epon-embedding mixture

solution A	3.5 ml
solution B	6.5 ml
para-dimethyl aminomethyl phenol (Serva, Germany)	0.15 ml

Azur II/Safranin staining protocol for semithin sections

Azur II solution

Disodium tetraborate (Merck 6306, Germany)	1.0 g
Aqua dest.	100 ml
Azur II (Merck 9211, Germany)	1.0 g
37% Formaldehyde (Roth, Germany)	250 µl

Dissolve borate in aqua dest., then add Azur II and stir for approximately two hours before adding formaldehyde. Filter prior to use.

Safranin O solution

Disodium tetraborate (Merck 6306, Germany)	1.0 g
Aqua dest.	100 ml
Safranin O (Chroma 1B 463, Germany)	1.0 g
Saccharose (Merck, Germany)	40.0 g
37% Formaldehyde (Roth, Germany)	250 µl

Dissolve borate in aqua dest., then add Safranin and saccharose. Stir for approximately two hours before adding formaldehyde. Filter prior to use. Stain sections in Azur II solution for 15-20 seconds at 55°C on a heating plate (Meditel, Germany) and rinse with distilled water. Dry. Then stain sections for 15-20 seconds at 55°C on a heating plate (Meditel, Germany) and rinse with distilled water. Dry. Cover sections with glass coverslips (Menzel GmbH & Co KG, Germany) using Histofluid® (Superior, Germany).

3.8.4. Quantitative stereological analyses

3.8.4.1 Estimation of the mean glomerular volume

The kidney volume was calculated dividing the kidney weight by the specific weight of mouse kidneys (1.05 mg/mm^3) (Wanke 1996). The mean glomerular volume was estimated, using a model-based method, as previously described in detail(Hirose et al., 1982, Wanke 1996, Weibel and Gomez 1962). In this model-based stereological approach, the glomeruli were considered as rotation ellipsoids. The mean glomerular area was obtained from planimetric measurements of glomerular profile areas. In the calculation, a shape coefficient and a size distribution coefficient were considered. The results were corrected for embedding shrinkage. The values for the shape and size distribution coefficient as well as for the shrinkage correction factor for plastic embedded murine renal tissue were taken from Wanke (1996). Morphometric evaluation was carried out on a Videoplan® image analysis system (Zeiss-Kontron, Germany) coupled to a light microscope (Orhoplan; Leitz, Germany) via a color video camera (CCTV WV-CD132E; Matsushita, Japan). Images of PAS stained GMA/MMA-embedded sections were displayed on a color monitor at a 400x final magnification. The profiles of about 100 glomeruli per animal (mean 105 ± 5) were measured planimetrically by circling their contours with a cursor on the digitizing tablet of the image analysis system after calibration with an object micrometer (Zeiss, Germany).

The stereologically estimated mean glomerular volume was calculated as the product of the mean glomerular area to the power of 1.5 and the shape coefficient (ß=1.40), divided by the size distribution coefficient (k=1.04) (Weibel 1980). Results were corrected for embedding shrinkage, using the linear tissue shrinkage correction factor (fs = 0.91) for murine kidney tissue embedded in GMA/MMA (Wanke 1996):

$$\bar{v}_{Glom} = \frac{\beta}{k} * \overline{A}_{Glom}^{1.5} / fs^3$$

3.8.4.2. Estimation of the mean glomerular mesangium and capillary volumes

The mesangial and capillary volume fractions ($Vv_{(Mes/Glom)}$ and $Vv_{(Cap/Glom)}$, respectively) were determined on PAS-stained plastic sections by point counting, using a computer-assisted stereology system (NewCast, Visiopharm, Denmark) at the age of 1 and 6 months. The sum of all points hitting mesangium or capillaries was divided by the sum of points hitting glomeruli. On the average 40 whole glomeruli (range 30-46) were evaluated (corresponding to 265-670 reference points). The mean glomerular mesangium or capillary volumes ($v_{(Mes,Glom)}$ and $v_{Cap,Glom)}$, respectively) were obtained by multiplying the respective volume fraction by $\bar{v}_{(Glom).}$

3.8.4.3. Estimation of total numbers and mean volumes of podocytes

The number of podocytes per glomerulus was estimated by applying the physical disector principle at the age of 1 and 6 months. The disector is a three dimensional stereologic probe, which allows unbiased and assumption free counting and sizing of particles (Sterio 1984). The physical disector, which consists of a pair of physical section planes separated by a known distance, was used to estimate the numerical density of podocytes. In each case eight serial semithin sections (nominal thickness 0.5 µm) of the Epon-embedded samples of cortical kidney tissue were cut with an Ultracut E microtome (Leica, Germany), mounted on glass slides and stained with Azur II/Safranin. Photographs of complete profiles of identical glomeruli, present in the centre of two semithin sections (reference section and look-up section; disector height: 1.5 µm), were taken at a magnification of x 400 using a Leica DFC 320 camera (Leica, Germany) connected to a microscope (Orthoplan, Leitz, Germany). At the beginning of each set, an object micrometer (Zeiss, Germany) was photographed under the same conditions for calibration. Prints of all pictures were made at a constant setting of the enlarger. Prints of pictures of nine pairs of glomerular profiles

from each animal were analyzed. The areas of the glomerular profiles were measured planimetrically on these prints by circling their contours with a cursor on the digitizing tablet of the image analysis system (Zeiss-Kontron, Germany) after calibration. All nuclei of podocytes (P) sampled in the reference section, which were not present in the look-up section, were counted ($Q^-_{(P)}$). The process of counting was then repeated by interchanging the roles of the reference and look-up section, thereby increasing the efficiency by a factor of two.

The numerical density of podocytes in glomeruli was calculated as

$N_{V(P/Glom)} = \frac{\sum Q^-_{(P)}}{h \times \sum A_{(Glom)}} \times fs^3$ where h was the disector height (1.5 µm) and fs the linear tissue shrinkage correction factor for Epon embedded murine kidney tissue (0.95) (Wanke 1996).

The number of podocytes per glomerulus ($N_{(P,Glom)}$) was calculated multiplying $N_{V(P/Glom)}$ and $\bar{v}_{(Glom)}$.

The volume fraction of podocytes per glomerulus ($Vv_{(P/Glom)}$) was determined by point counting method. The mean podocyte volume ($\bar{v}_{(P)}$) was calculated dividing $Vv_{(P/Glom)}$ by $N_{V(P/Glom)}$.

3.9 Data presentation and statistical analysis

Data is presented as means ± SEM or SD as indicated. Statistical significance of differences between two groups was calculated by one-way ANOVA and LSD test, using GraphPad Prism 5.0 (GraphPad Software, Inc, USA). P values < 0.05 were considered significant. The albumin-to-creatinine ratios (ACR) were logarythmized to normalize their distribution (van Goor et al., 1991).

4. Results

4.1 Body weight

Body weights were determined from 1 month of age onwards in 2-week intervals. From about 2 to 6 months of age, the body weight of transgenic animals was significantly lower than that of control mice. Uninephrectomy had no influence on body weights of transgenic or control mice vs. the respective sham operated counterparts (Fig. 4.1)

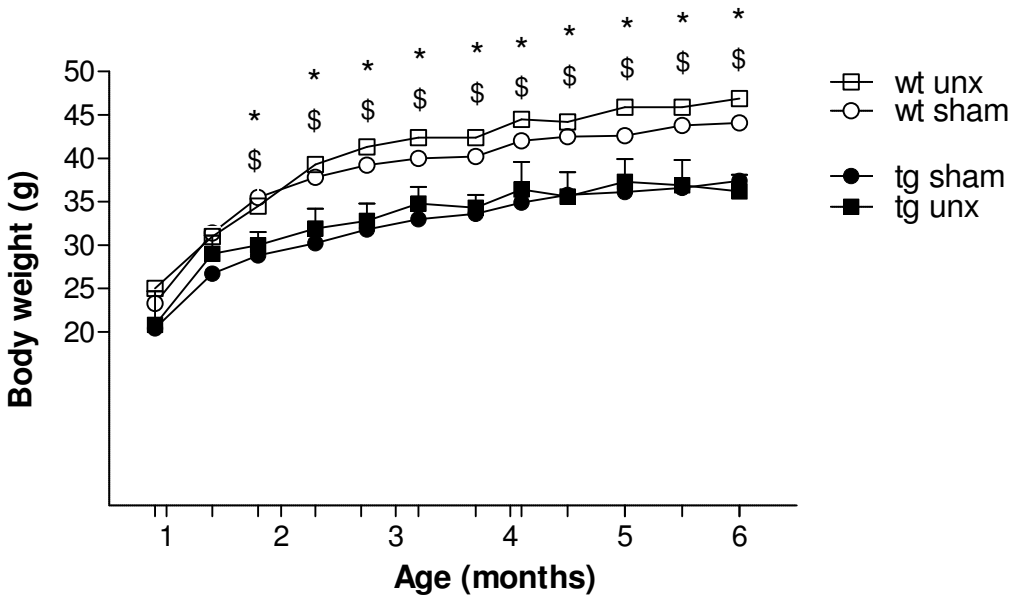

Fig. 4.1.: Body weights of uninephrectomized (unx) and sham operated (sham) transgenic (tg) and wild-type (wt) mice.
Data are means and SEM; n ≥ 5/group; * p<0.05 wt sham vs. tg sham; $ p<0.05 wt unx vs. tg unx.

4.2 Blood pressure

Systolic and diastolic blood pressure did not differ between the groups irrespective of the age at sampling (Fig. 4.2.).

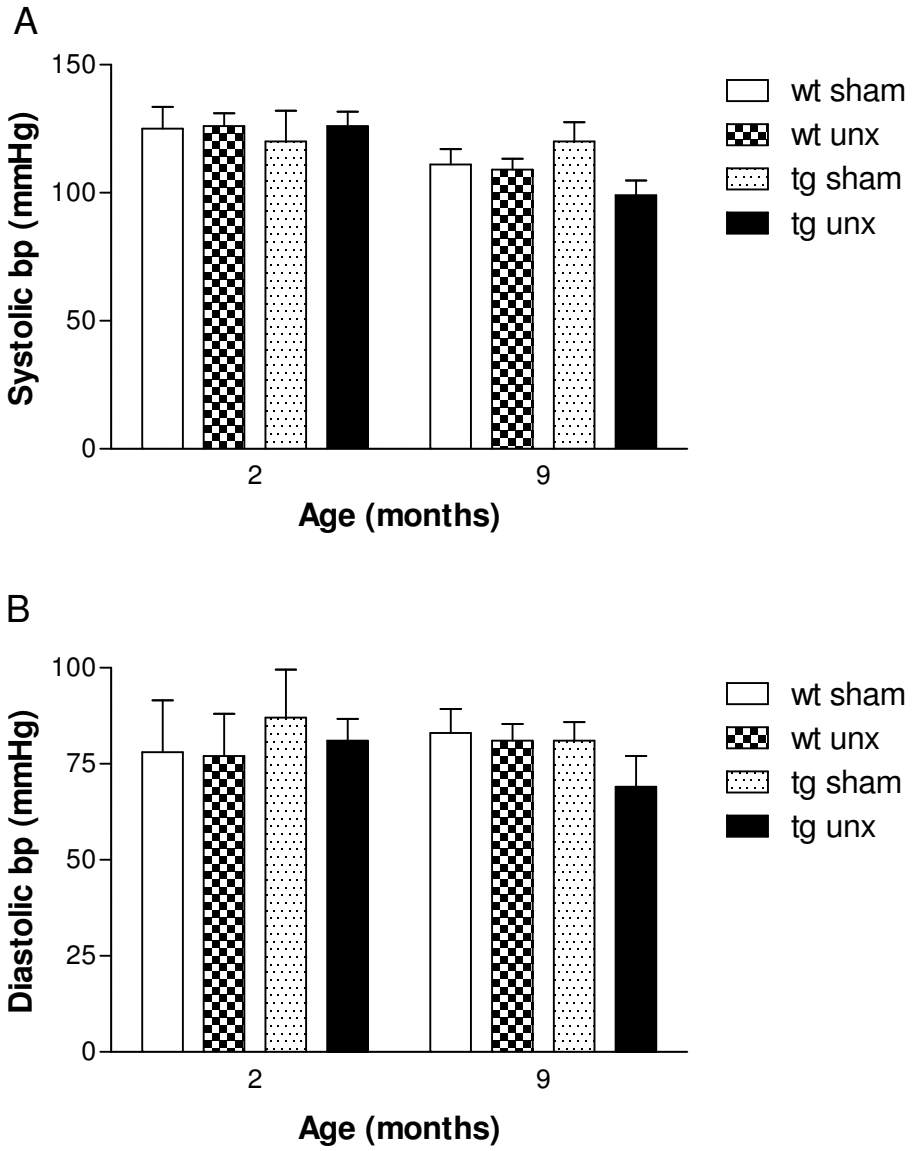

Fig. 4.2.: Systolic (A) and diastolic (B) blood pressure of uninephrectomized (unx) and sham operated (sham) transgenic (tg) and wild-type (wt) mice at 2 and 9 months of age.

Data are means and SEM, n ≥ 4/group

4.3 Blood and serum glucose

Blood glucose levels of 21-day-old transgenic mice were significantly higher than those of control mice. There was no difference in blood glucose levels between animals that were to be sham operated or uninephrectomized in either the wild-type or the transgenic group (Fig. 4.3).

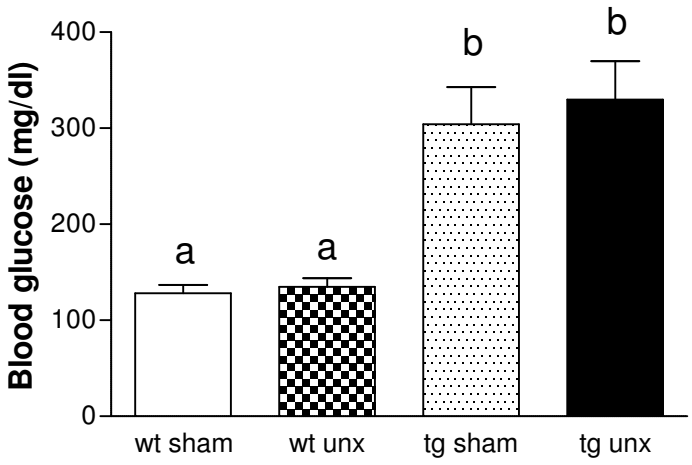

Fig. 4.3: Blood glucose levels at 21 days of age of transgenic (tg) and wild-type (wt) mice that were selected for either future uninephrectomy (unx) or sham operation (sham). Data are means and SEM, different superscripts indicate significant differences between groups. n ≥ 5/group.

Serum glucose levels of transgenic mice were significantly higher than those of wild-type mice; Uninephrectomy had no influence on serum glucose concentrations of either transgenic or control mice (Table 4.1).

group / age	4 months	6 months	12 months
wt sham	167 ± 25	164 ± 33	135 ± 38
wt unx	165 ± 30	151 ± 15	108 ± 37
tg sham	804 ± 89*	819 ± 68*	790 ± 147*
tg unx	809 ± 162$	850 ± 201$	778 ± 191$

Table 4.1 Serum glucose concentrations (mg/dl) of sham operated (sham) and uninephrectomized (unx) transgenic (tg) and wild-type (wt) mice at 4, 6 and 12 months of age. Data are means and SD; n=6 animals/group; * $p<0.05$ wt sham vs. tg sham; $ $p<0.05$ wt unx vs. tg unx.

4.4 Serum parameters

The serum samples of all animals at four, six, and twelve months of age were screened for chloride, total protein, creatinine, urea, triglyceride, and albumin.
Serum urea, creatinine and triglycerides of sham operated and uninephrectomized transgenic animals were slightly or significantly increased and total protein, albumin and chloride levels were slightly or significantly decreased vs. the respective controls, irrespective of the age at sampling. Uninephrectomized wild-type and transgenic mice exhibited slightly higher urea levels vs. the respective sham operated mice.

Group	Urea (mg/dl)	Creatinine (mg/dl)	TG (mg/dl)	Total protein (g/l)	Albumin (g/l)	Chloride (mmol/l)
4 months						
wt sham	58 ± 12	0.4 ± 0.0	101 ± 61	5.8 ± 0.2	3.4 ± 0.2	111 ± 4
wt unx	80 ± 17	0.5 ± 0.1§	108 ± 79	5.7 ± 0.2	3.3 ± 0.2	109 ± 5
tg sham	89 ± 39	0.6 ± 0. 1*	149 ± 70	5.2 ± 0.3*	3.0 ± 0.2*	106 ± 6*
tg unx	99 ± 44	0.7 ± 0.1$^{\$}$	188 ± 104$^{\$}$	5.0 ± 0.4$^{\$}$	2.8 ± 0.4$^{\$}$	107 ± 6
6 months						
wt sham	67 ± 19	0.4 ± 0.0	85 ± 21	5.3 ± 0.3	3.2 ± 0.2	111 ± 2
wt unx	88 ± 18	0.4 ± 0.0	129 ± 42	5.1 ± 0.5	3.2 ± 0.2	109 ± 4
tg sham	85 ± 24	0.6 ± 0.1*	184 ± 113*	4.9 ± 0.4	2.8 ± 0.2*	104 ± 4*
tg unx	103 ± 26	0.5 ± 0.1$^{\$\%}$	196 ± 55	4.6 ± 0.3$^{\$}$	2.7 ± 0.2$^{\$}$	100 + 0$^{\$}$
12 months						
wt sham	61 ± 12	0.4 ± 0.0	105 ± 33	5.8 ± 0.2	3.5 ± 0.2	108 ± 1
wt unx	66 ± 33	0.4 ± 0.1	224 ± 273	5.4 ± 1.8	3.0 ± 1.0	95 ± 25
tg sham	65 ± 8	0.6 ± 0.2*	211 ± 48*	5.4 ± 0.2*	3.0 ± 0.2*	108 ± 5
tg unx	82 ± 31	0.8 ± 0.1$^{\$\%}$	180 ± 30	5.3 ± 0.1	3.0 ± 0.0	107 ± 1

Table 4.2 Serum parameters of sham operated (sham) and uninephrectomized (unx) transgenic (tg) and wild-type (wt) mice at 4, 6 and 12 months of age. Data are means and SD; n= 6 animals/group; TG, triglycerides; * $p<0.05$ wt sham vs. tg sham; $ $p<0.05$ wt unx vs. tg unx § $p<0.05$ wt vs. wt; % $p<0.05$ tg vs. tg.

4.5 Urine analyses

GIPR^{dn} transgenic mice exhibited selective glomerular proteinuria at 4 and 5 months of age compared to their corresponding non transgenic littermate controls. Bands of approximately 69 kDa, which meets the size of murine albumin, were detected by SDS-PAGE. Excretion of proteins larger than 37 kDa was not detectable in the urine samples of controls. Bands in the region of approximately 18 kDa reflect major urinary proteins (MUPs), which appear in the murine urine under physiological conditions particularly in male mice.

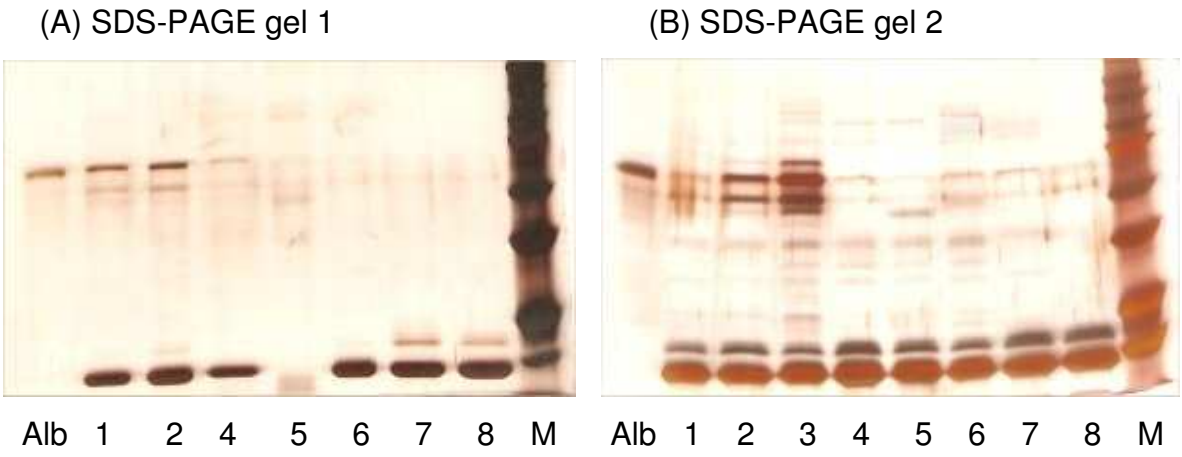

Fig. 4.4.: (A/B) SDS-PAGE of urine samples of uninephrectomized GIPR^{dn} transgenic (# 1-3), sham operated transgenic (# 4-6), sham operated control (# 7), and uninephrectomized control (# 8) mice at (A) 4 and (B) 5 months of age.

Alb: Mouse albumin standard, M: Precision Protein Standard (BIORAD, Germany), molecular weight from top to bottom: 250, 150, 100, 75, 50, 37, 18 kDa.

Urinary albumin and creatinine concentrations were determined from 1 until 6 months of age in about monthly intervals and the albumin-to-creatinine ratio (ACR) was calculated. Urinary creatinine levels of transgenic mice were significantly lower than those of wild-type mice from about one and a half months of age onwards (Fig. 4.5).

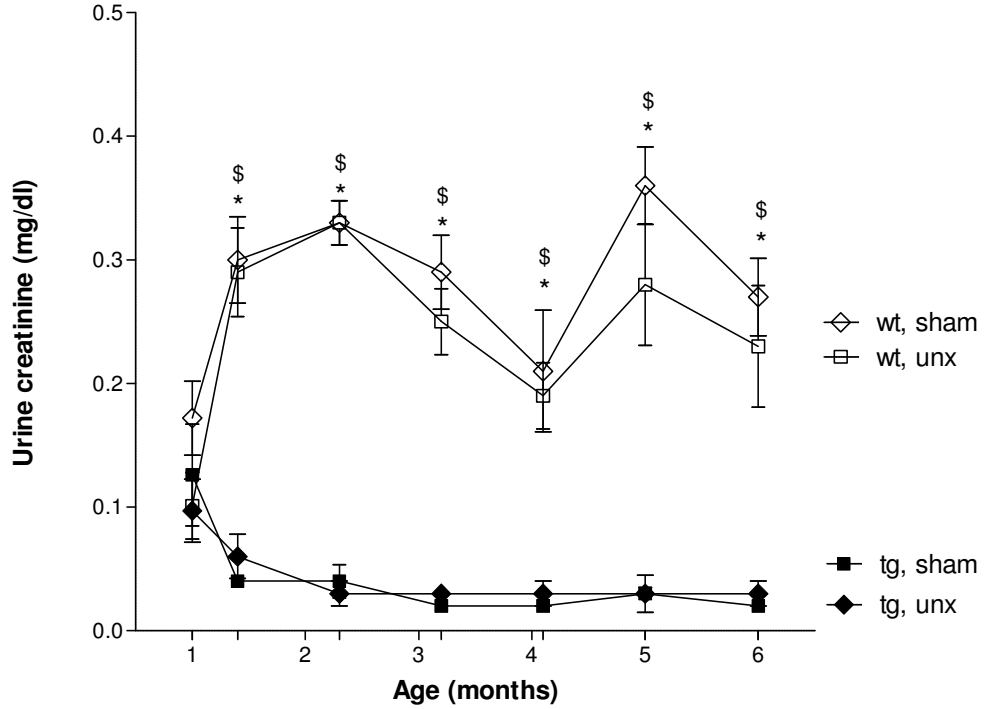

Fig. 4.5. Urinary creatinine concentrations of sham operated (sham) and uninephrectomized (unx) transgenic (tg) and wild-type (wt) mice between 1 and 6 months of age. Data are means and SEM; n ≥ 4/group; * $p<0.05$ wt sham vs. tg sham; $ $p<0.05$ wt unx vs. tg unx

From about 2 months of age, both uninephrectomized and sham operated transgenic mice exhibited a higher ACR as compared to the respective control mice. The ACR of sham operated transgenic mice was increased up to 3-fold, that of uninephrectomized transgenic mice was increased up to 92-fold vs. the respective wild-type mice. In addition, uninephrectomized transgenic mice showed a significantly higher ACR vs. sham operated $GIPR^{dn}$ transgenic mice. Uninephrectomy had no influence on the ACR of wild-type mice (Fig. 4.6).

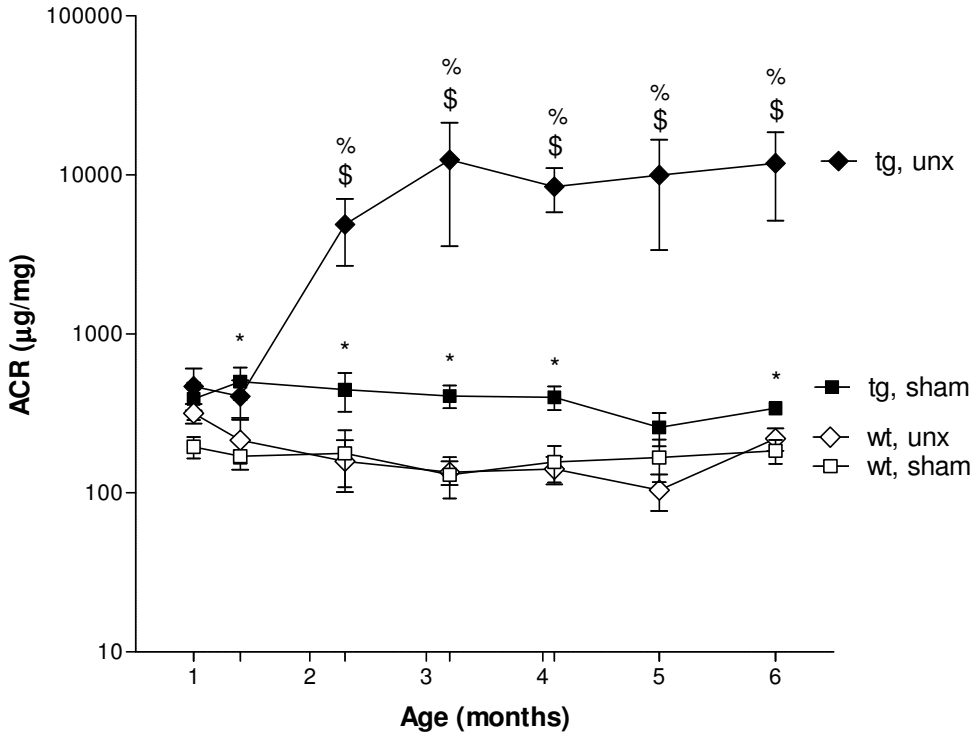

Fig. 4.6. Urinary albumin-to-creatinine ratio (ACR) of sham operated (sham) and uninephrectomized (unx) transgenic (tg) and wild-type (wt) mice between 1 and 6 months of age. Time of operation was at 1 month. Data are means and SEM; n ≥ 4/group; * $p<0.05$ wt sham vs. tg sham; $ $p<0.05$ wt unx vs. tg unx; % $p<0.05$ tg vs. tg

At 4 months of age, 24 hour urine was collected and the ACR in 24 hour urine samples was calculated. The urine volume of transgenic animals was significantly higher that that of the respective control mice, irrespective of the kind of operation (Fig. 4.7). Uninephrectomized and sham operated transgenic mice exhibited significantly higher ACR in 24 hour urine samples than the corresponding control mice. The ACR in 24 hour urine samples of sham operated transgenic mice was increased 700-fold, that of uninephrectomized transgenic mice was increased 400-fold vs. the respective wild-type controls. Uninephrectomized transgenic mice showed a significantly higher ACR in 24 hour urine samples than sham operated transgenic animals (Fig. 4.8.).

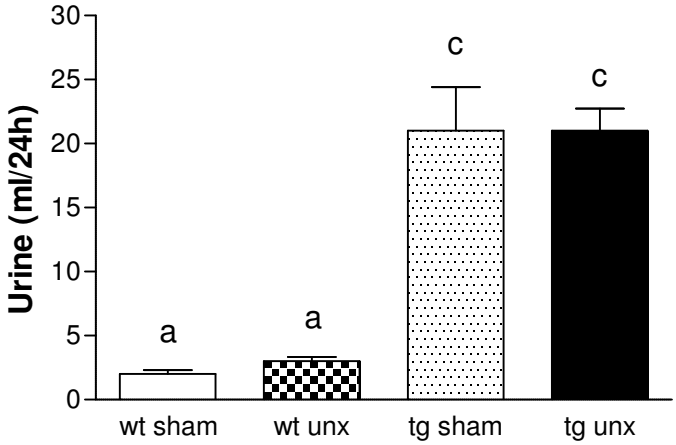

Fig. 4.7. Daily urine volume of sham operated (sham) and uninephrectomized (unx) transgenic (tg) and wild-type (wt) mice at 4 months of age. Data are means and SEM; n ≥ 6/group; Different superscripts indicate significant differences between groups ($p<0.05$)

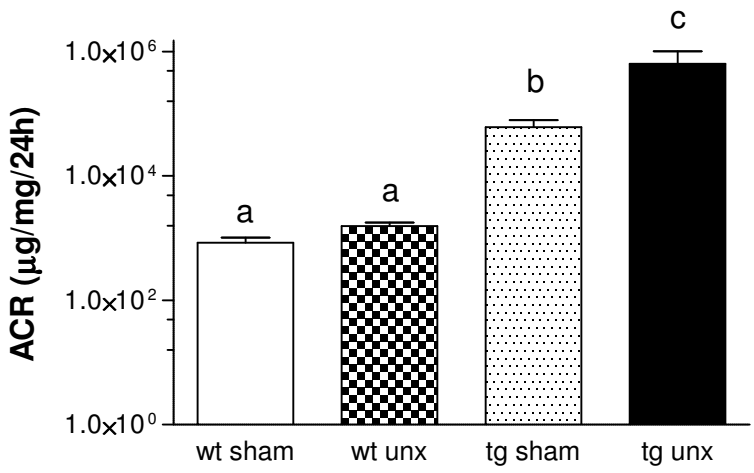

Fig. 4.8 Albumin-to-creatinine ratio (ACR) in 24 hour urine samples of sham operated (sham) and uninephrectomized (unx) transgenic (tg) and wild-type (wt) mice at 4 months of age; Data represent means and SEM; n ≥ 6/group; Different superscripts indicate significant differences between groups ($p<0.05$)

4.6 Glomerular filtration rate

The glomerular filtration rate (GFR) was calculated from urine creatinine, urine volume and serum creatinine at 4 months of age. Both uninephrectomized and sham operated $GIPR^{dn}$ transgenic mice showed a significantly reduced GFR vs. the respective control mice. The GFR of uninephrectomized transgenic mice was

significantly lower than that of sham operated transgenic mice. In wild-type mice, uninephrectomy did not influence the GFR (Fig 4.9).

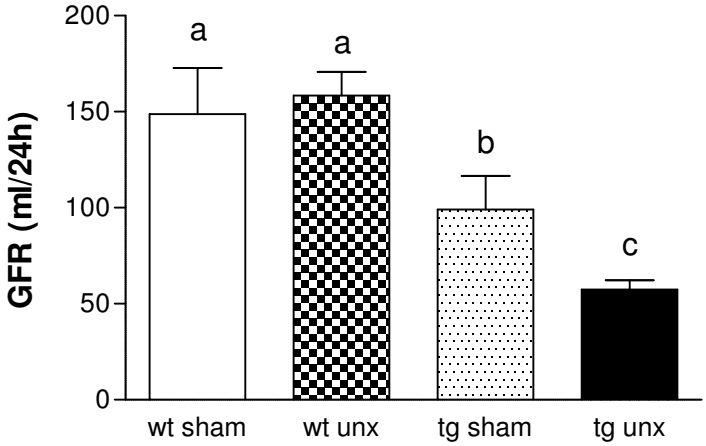

Fig. 4.9. Glomerular filtration rate (GFR) of sham operated (sham) and uninephrectomized (unx) transgenic (tg) and wild-type (wt) mice at 4 months of age; Data represent means and SEM; Different superscripts indicate significant differences between groups ($p<0.05$)

4.7 Qualitative histological findings of the kidneys

The uninephrectomized left kidneys of 1-month-old transgenic mice did not show macroscopical or histological abnormalities vs. wild-type mice. The kidneys of 6- and some 12-month-old transgenic mice appeared enlarged and the renal pelvis was sometimes slightly dilated vs. wild-type mice. In addition, the ureters and bladders of transgenic animals were frequently dilated as compared to wild-type mice. There were no differences in these macroscopical aspects comparing uninephrectomized and sham operated transgenic mice. One uninephrectomized $GIPR^{dn}$ transgenic mouse aged about 7 months showed renal atrophy with a granular kidney surface (Fig. 4.10). The kidneys of uninephrectomized wild-type mice appeared larger than those of sham operated control mice.

Histologically, glomeruli of 6- and 12-month-old $GIPR^{dn}$ transgenic mice appeared enlarged, showed focal to diffuse segmental to panglomerular mesangial expansion, focal glomerulosclerosis, synechia between the glomerulus, and the capsule of Bowman and large distorted capillaries. Tubulo-interstitial lesions of transgenic mice included protein reabsorption droplets in proximal tubular epithelia, proteinaceous casts in distal tubules, focal tubular atrophy and few focal interstitial mononuclear

inflammatory cell infiltrates. The mentioned glomerular and tubulo-interstitial changes were more severe in some 12-month-old uninephrectomized transgenic mice vs. 6-month-old transgenic mice. The single uninephrectomized GIPR^{dn} transgenic mouse exhibiting the atrophic kidney mentioned above showed diffuse panglomerular glomerulosclerosis and glomerular hyalinosis with numerous obsolescent glomeruli, and focal cystic dilation of the capsule of Bowman. In addition, multiple tubular cysts, severe interstitial fibrosis with mononuclear infiltrates, pigment laden macrophages and signs of proteinuria were evident. Both sham operated and uninephrectomized wild-type mice developed focal segmental mesangium expansion and few foci of interstitial fibrosis with lymphoplasmacellular infiltrates, these changes being more severe in 12- than in 6-month old wild-type mice and more pronounced in uninephrectomized vs. sham operated wild-type mice. Some glomeruli of 12-month-old uninephrectomized wild-types showed large distorted capillaries. Proteinaceous casts and tubular atrophy were rarely observed in wild-type mice (Figures 4.11 A-P).

Fig. 4.10 Perfusion fixed kidney of an about 7-month-old uninephrectomized GIPR^{dn} transgenic mouse that is unusually small (300 mg vs. about 600 to 1000 mg in other uninephrectomized transgenic mice) and exhibits a granular surface.

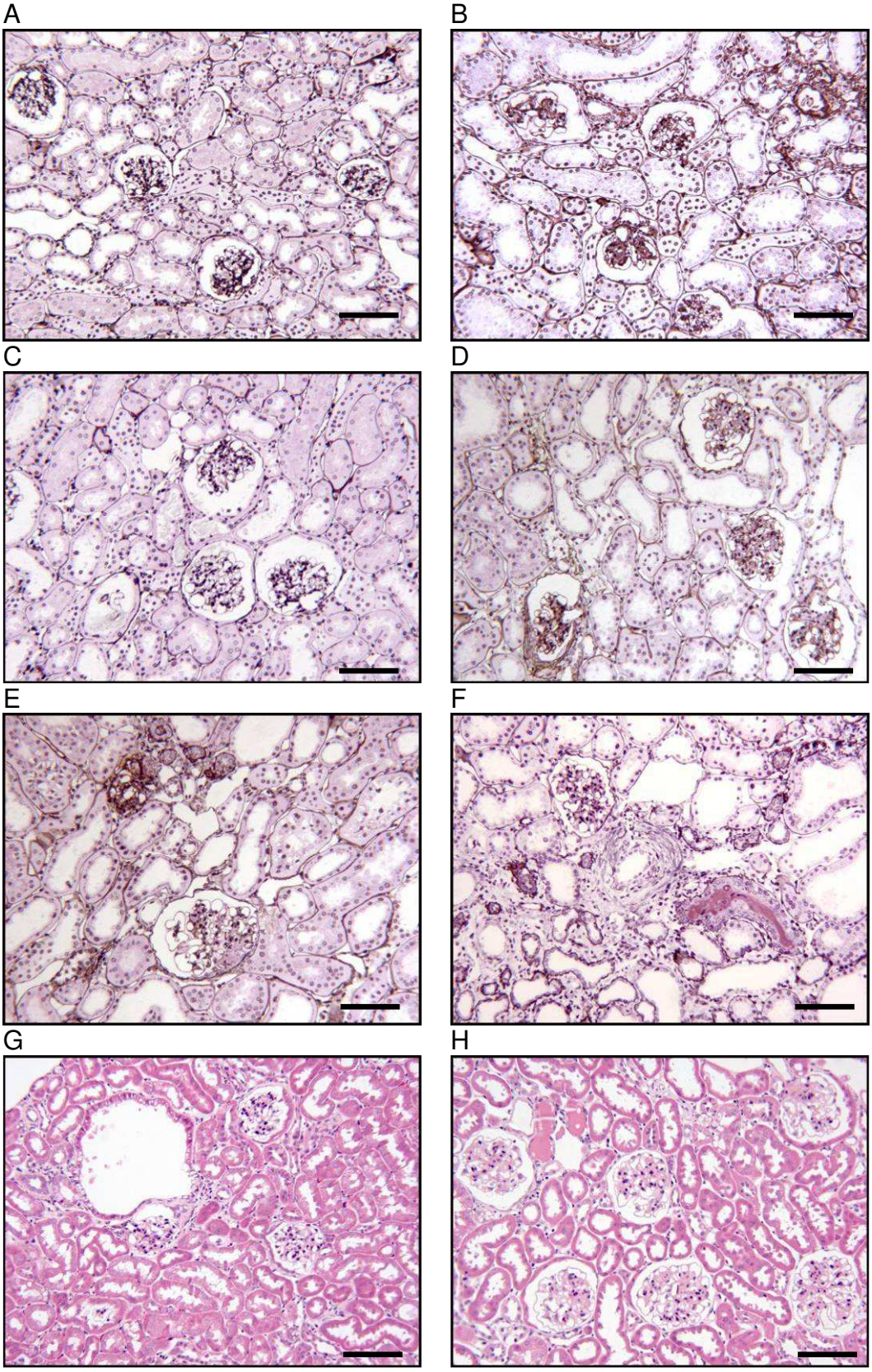
A
B
C
D
E
F
G
H

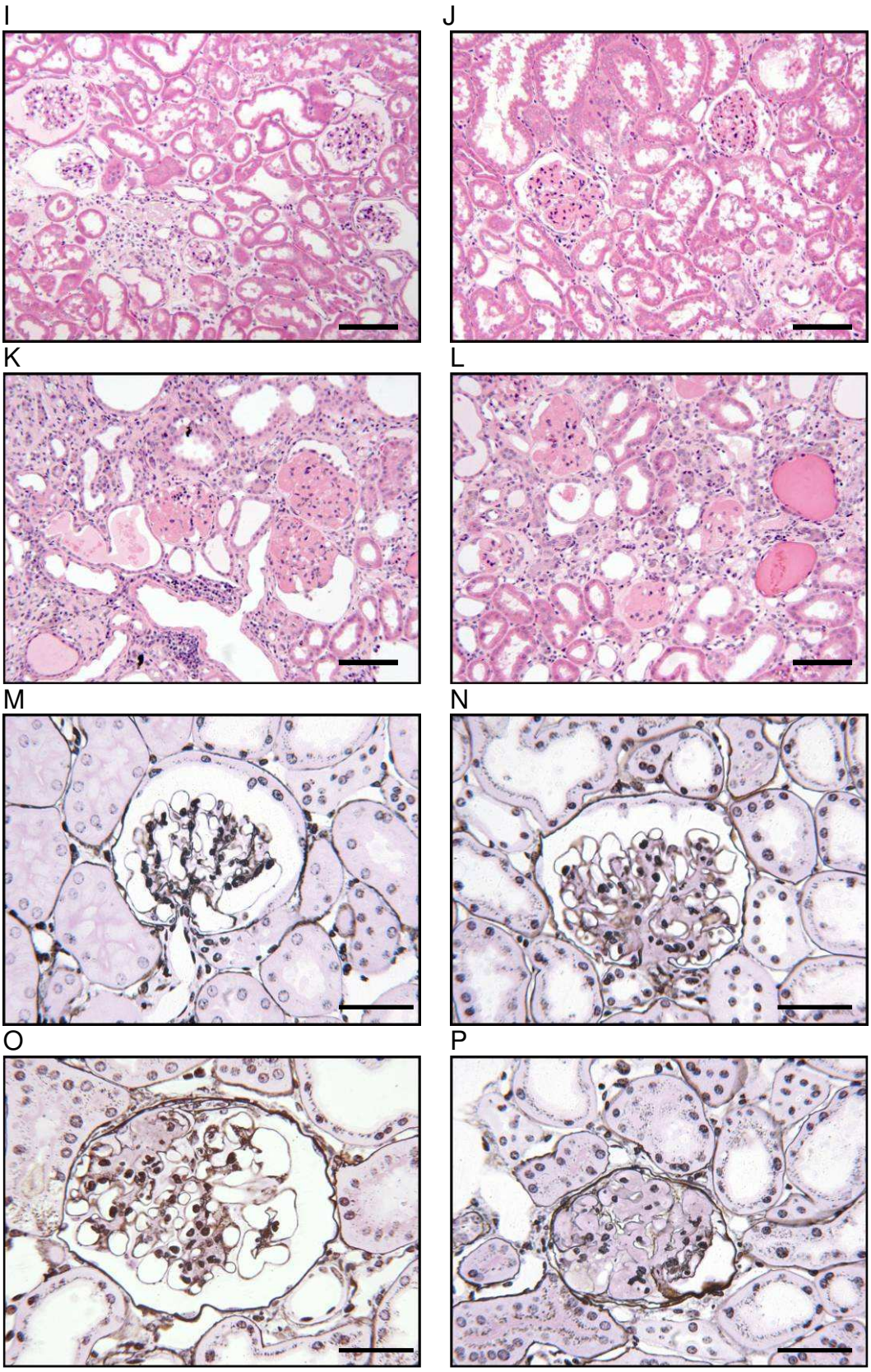

Fig. 4.11 Histology of the kidneys of sham operated (sham) and uninephrectomized (unx) transgenic (tg) and wild-type (wt) mice at 6 (A-F, M-P), 12 (G-J) and 7 months

of age (K,L). A) wt sham showing normal renal architecture; B) tg sham showing mesangial expansion and tubular atrophy (top right); C) wt unx showing glomerular hypertrophy; D-F) tg unx, showing mesangium expansion and synechia between the glomerular tuft and the capsule of Bowman (in D,E), tubular atrophy and signs of proteinuria (in F); G) wt sham showing a tubular cyst; H) tg sham, showing mesangial expansion signs of proteinuria, and a small focus of interstitial fibrosis; I) wt unx showing focal interstitial fibrosis and mononuclear cell infiltration; J-L) tg unx showing panglomerular mesangial expansion, focal fibrosis (in J), glomerulosclerosis with sometimes glomerular obsolescence, dilated tubules with proteinaceous casts, interstitial fibrosis, mononuclear infiltration and pigment laden cells (in K,L); M-P glomerular profiles of M) wt, unx without pathological changes; N) tg sham demonstrating mesangial expansion and matrix accumulation; O) tg unx showing segmental glomerulosclerosis with synechia formation; P) tg unx exhibiting glomerular obsolescence due to hyalinosis; Bar in A-L 100 μm, in M-P 50 μm; A-F, M-P) PASM-PAS stained plastic sections; G-L) H&E-stained plastic sections

4.8. Quantitative stereological findings of the kidneys

4.8.1 Kidney volume

The kidney volumes of the uninephrectomized left kidneys (age 1 month) and of the kidney remnant or the right kidneys of sham operated animals (age 6 and 12 months) was determined. At time of uninephrectomy, there were no differences in kidney weights of transgenic and control mice. At 6 months of age, the kidney volumes of uninephrectomized and sham operated transgenic mice were significantly higher than those of their respective controls. Uninephrectomy led to a significantly increased kidney volume vs. sham operation in both 6-month-old GIPR^{dn} transgenic and wild-type mice. The kidney volumes of 12-month-old uninephrectomized wild-type mice were significantly higher than those of age-matched sham operated controls. There were no differences in the kidney volumes of transgenic mice vs. controls or between the two transgenic groups at 12 months of age. (Fig. 4.12)

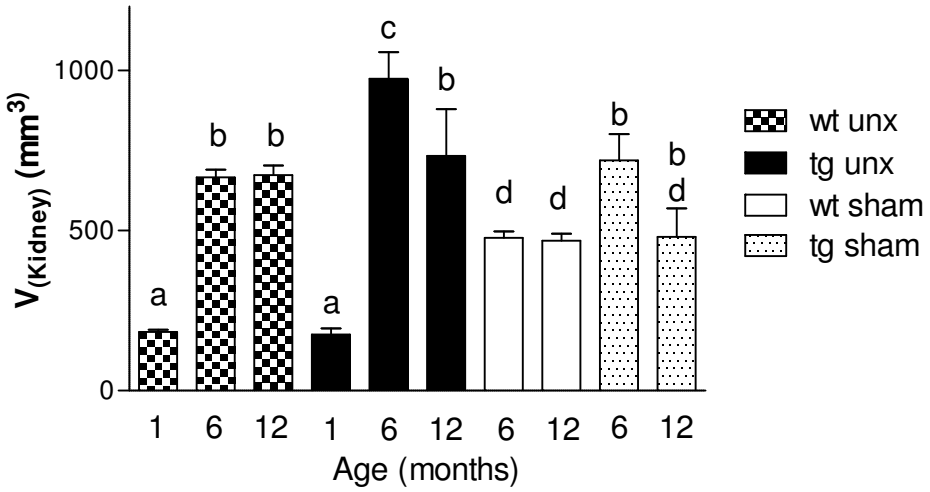

Fig. 4.12. Kidney volumes of sham operated (sham) and uninephrectomized (unx) transgenic (tg) and wild-type (wt) mice at 1, 6 and 12 months of age; Data represent means and SEM; Different superscripts indicate significant differences between groups ($p<0.05$). Data at 1 month of age represent kidney volumes of the removed left uninephrectomized kidney, data of uninephrectomized animals at 6 months of age are kidney volumes of the right kidneys of the same animals.

4.8.2 Mean glomerular volume

The mean glomerular volume of the uninephrectomized left kidneys (age 1 month) and of the kidney remnant or the right kidneys of sham operated animals (age 6 and 12 months) was determined, using quantitative stereological techniques.

At time of uninephrectomy, there were no differences in the mean glomerular volumes, comparing transgenic and control mice. At 6 months of age, the mean glomerular volumes of uninephrectomized and sham operated transgenic mice were significantly higher than those of their respective controls. Uninephrectomy led to a significantly higher mean glomerular volume vs. sham operation in both $GIPR^{dn}$ transgenic and wild-type mice, and uninephrectomized wild-type mice exhibited an equal mean glomerular volume as sham operated transgenic mice. At 12 months of age, sham operated transgenic animals exhibited a higher mean glomerular volume vs. sham operated wild-type mice and uninephrectomized wild-type mice displayed a significantly higher mean glomerular volume as compared to sham operated wild-type mice. Uninephrectomized and sham operated 12-month-old transgenic and uninephrectomized wild-type showed equal mean glomerular volumes. The mean glomerular volume increased significantly in both uninephrectomized wild-type and transgenic animals from 1 to 6 months of age. Sham operated 12-month-old transgenic animals exhibited a significantly higher mean glomerular volume vs. their 6-month-old counterparts, in all other groups the mean glomerular volume did not change between 6 and 12 months of age. Interestingly, uninephrectomy of wild-type mice led to a similar degree of glomerular hypertrophy as hyperglycemia in sham operated $GIPR^{dn}$ transgenic mice (Fig. 4.13).

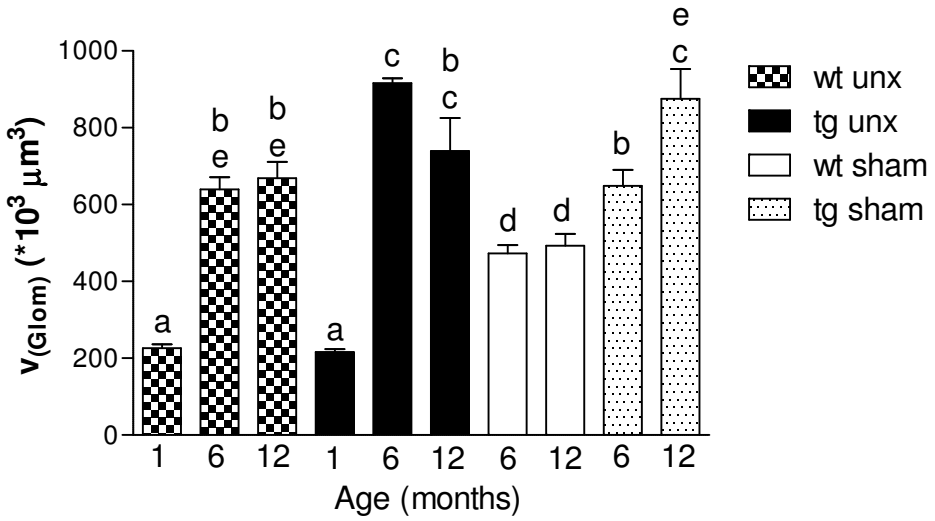

Fig 4.13. Mean glomerular volume of sham operated (sham) and uninephrectomized (unx) transgenic (tg) and wild-type (wt) mice at 1, 6 and 12 months of age; Data represent means and SEM; Different superscripts indicate significant differences between groups ($p<0.05$). Data at 1 month of age represent mean glomerular volumes of the removed left kidney, data of uninephrectomized animals at 6 months of age are mean glomerular volumes of the right kidneys of the same animals.

4.8.3 Volume densities of capillaries and mesangium per glomerulus and mean glomerular mesangium and capillary volumes

The volume densities of mesangium and capillaries per glomerulus were not different between groups (Table 4.3).

Group	$Vv_{(Mes/Glom)}$ (%)	$Vv_{(Cap/Glom)}$ (%)
1 month		
wt unx (6)	41 ± 6	32 ± 5
tg unx (6)	42 ± 5	35 ± 5
6 months		
wt unx (6)	40 ± 7	33 ± 4
tg unx (6)	37 ± 7	38 ± 5
wt sham (6)	38 ± 6	37 ± 7
tg sham (6)	37 ± 6	36 ± 5

Table 4.3 Volume densities of mesangium ($Vv_{(Mes/glom)}$ and capillaries ($Vv_{(Cap/Glom)}$ per glomerulus of sham operated (sham) and uninephrectomized (unx) transgenic (tg) and wild-type (wt) mice at 1 and 6 months of age. (n), number of animals investigated; data are means and SD;

The mean glomerular mesangium volume ($v_{(Mes,Glom)}$) of 6-month-old transgenic mice was significantly higher than that of the respective controls. Uninephrectomy led to a significant increase of the $v_{(Mes,Glom)}$ of both transgenic and wild-type mice vs. the respective sham operated control animals. There was no difference between $v_{(Mes,Glom)}$ of uninephrectomized wild-type and sham operated transgenic animals, therefore uninephrectomy in healthy animals leads to the same extent of mesangial expansion as hyperglycemia. The $v_{(Mes,Glom)}$ increased significantly in both uninephrectomized wild-type and transgenic animals from 1 to 6 months of age (Fig. 4.14)

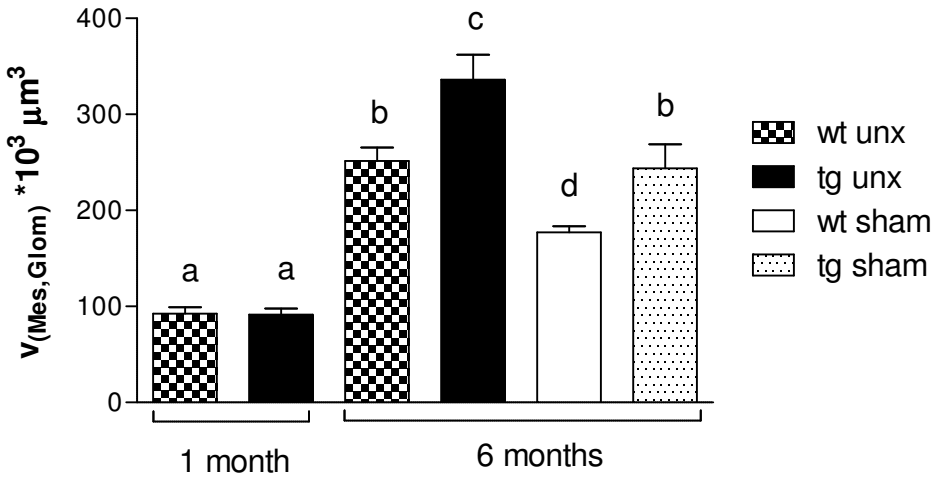

Fig 4.14. Mean glomerular mesangium volume of sham operated (sham) and uninephrectomized (unx) transgenic (tg) and wild-type (wt) mice at 1 and 6 months of age; Data represent means and SEM; Different superscripts indicate significant differences between groups ($p<0.05$) Data at 1 month of age represent mesangial volumes of the removed left kidney, data of uninephrectomized animals at 6 months of age are mesangial volumes of the right kidneys of the same animals.

The mean glomerular capillary volume ($v_{(Cap,Glom)}$) of 6-month-old transgenic mice was significantly higher than that of the corresponding controls. Uninephrectomy led to a significant increase of the $v_{(Cap,Glom)}$ of transgenic mice vs. sham operated transgenic animals. There was no difference in $v_{(Cap,Glom)}$ between uninephrectomized wild-type and sham operated wild-type or sham operated transgenic animals. The $v_{(Cap,Glom)}$ increased significantly in both uninephrectomized wild-type and transgenic animals from 1 to 6 months of age (Fig. 4.15)

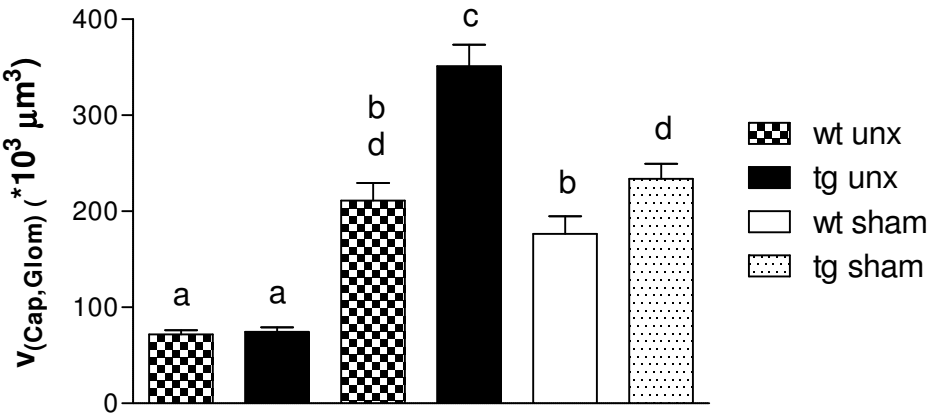

Fig 4.15. Mean glomerular capillary volume of sham operated (sham) and uninephrectomized (unx) transgenic (tg) and wild-type (wt) mice at 1 and 6 months of age; Data represent means and SEM; Different superscripts indicate significant differences between groups ($p<0.05$). Data at 1 month of age represent capillary volumes of the removed left kidney, data of uninephrectomized animals at 6 months of age are capillary volumes of the right kidneys of the same animals.

4.8.4 Numerical volume density of podocytes in glomeruli

The numerical volume density of podocytes in glomeruli ($Nv_{(Podo/Glom)}$) of 6-month-old transgenic mice was significantly lower than that of the respective wild-type mice. Uninephrectomy in wild-type mice led to a slight decrease of the $Nv_{(Podo/Glom)}$ vs. sham operated controls. The $Nv_{(Podo/Glom)}$ of uninephrectomized and sham operated transgenic mice did not differ. The $Nv_{(Podo/Glom)}$ significantly decreased from 1 to 6 months of age in both uninephrectomized wild-type and transgenic mice (Fig. 4.16).

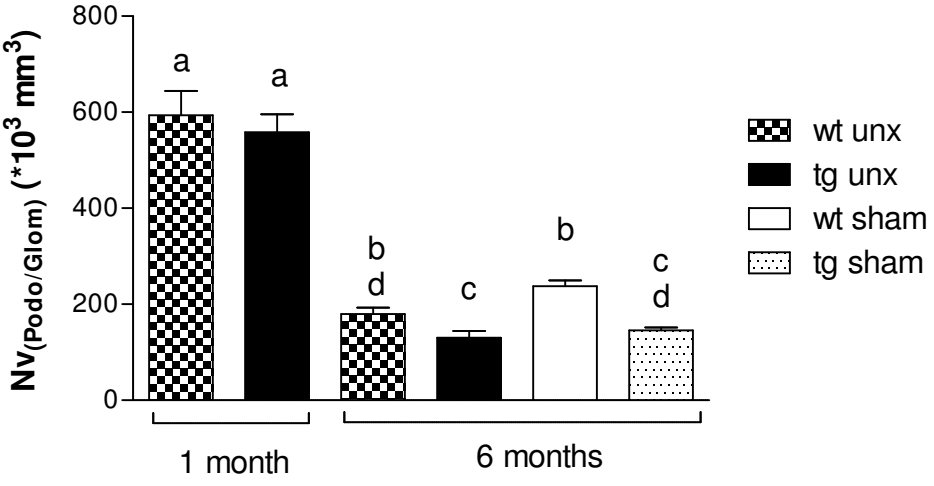

Fig. 4.16. Numerical volume density of podocytes in glomeruli of sham operated (sham) and uninephrectomized (unx) transgenic (tg) and wild-type (wt) mice at 1 and

6 months of age; Data represent means and SEM; Different superscripts indicate significant differences between groups ($p<0.05$). Data at 1 month of age represent numerical volume densities of podocytes of the removed left kidney, data of uninephrectomized animals at 6 months of age are numerical volume densities of podocytes of the right kidneys obtained from the same animals.

4.8.5 Total number and mean volume of podocytes

The total number of podocytes per glomerulus did not differ between the groups (Fig 4.17)

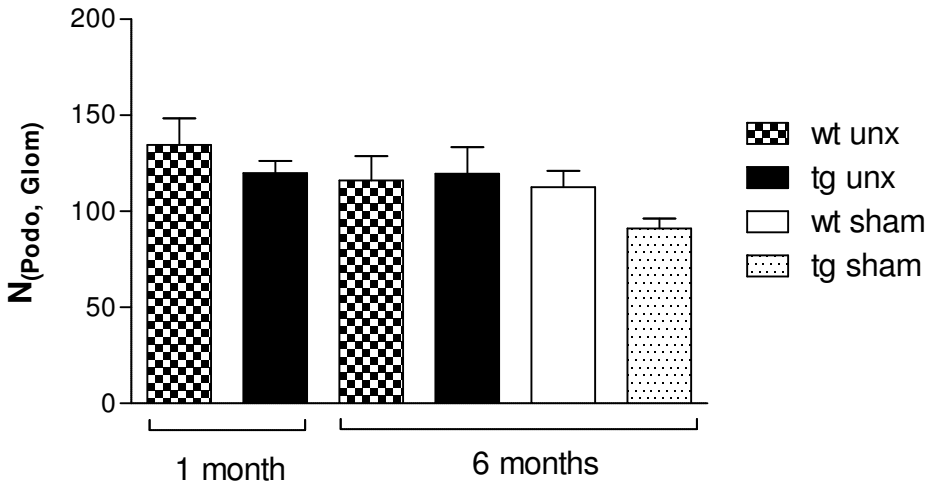

Fig. 4.17. Number of podocytes per glomerulus of sham operated (sham) and uninephrectomized (unx) transgenic (tg) and wild-type (wt) mice at 1 and 6 months of age; Data represent means and SEM; Different superscripts indicate significant differences between groups ($p<0.05$). Data at 1 month of age represent podocyte numbers of the removed left kidney, data of uninephrectomized animals at 6 months of age are podocyte numbers of the right kidneys obtained from the same animals.

The mean podocyte volume of 1-month-old transgenic and control mice did not differ. At 6 months of age, transgenic mice exhibited a significantly higher mean podocyte volume (podocyte hypertrophy) vs. the respective control mice. The mean podocyte volume of uninephrectomized wild-type mice was slightly higher than that of sham operated controls, but significantly lower than that of sham operated transgenic mice. Uninephrectomy did not lead to a significant increase of the mean podocyte volume of transgenic vs. sham operated transgenic mice (Fig. 4.18)

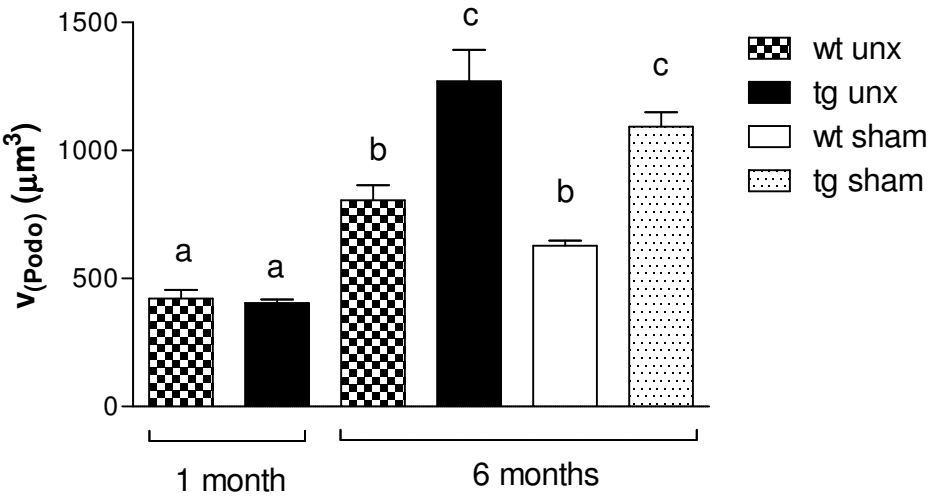

Fig. 4.18. Mean podocyte volume of sham operated (sham) and uninephrectomized (unx) transgenic (tg) and wild-type (wt) mice at 1 and 6 months of age; Data represent means and SEM; Different superscripts indicate significant differences between groups ($p<0.05$). Data at 1 month of age represent mean podocyte volumes of the removed left kidney, data of uninephrectomized animals at 6 months of age are mean podocyte volumes of the right kidneys obtained from the same animals.

5. Discussion

GIPR^{dn} transgenic mice were primarily designed in order to investigate the importance of the GIP (glucose dependent insulinotropic polypeptide) / GIP receptor axis for the enteroinsular axis *in vivo*. For this purpose, other mouse models had been generated before by means of gene targeting, including GIPR$^{-/-}$ mice and glucagon-like-peptide-1 receptor knockout (GLP-1R$^{-/-}$) mice, which both displayed only modest alterations in glucose homeostasis (Miyawaki et al., 1999, Scrocchi et al., 1996). The same was true for double mutant mice (GIPR$^{-/-}$/GLP-1R$^{-/-}$) (Hansotia et al., 2002, Preitner et al., 2002). A potential explanation for these unexpectedly mild phenotypic consequences was suggested to be compensation through other factors contributing to glucose homeostasis or the more complex alterations resulting from the knockout of incretin hormone receptors in all tissues (Baggio et al., 2000, Lewis et al., 2000, Pederson et al., 1998). To avoid these complicating mechanisms, the expression of a dominant negative mutant of the GIPR in transgenic mice was chosen as an alternative strategy to elucidate the role of the GIP receptor within the enteroinsular axis *in vivo* (Herbach et al., 2005, Volz 1997). The cDNA of the human GIPR was mutated at the third intracellular loop, where a deletion of eight amino acids (pos. 319-326) and a point mutation at position 340 was introduced. The loss of function of the mutated GIPR was demonstrated *in vitro*, using stably transfected CHL (Chinese hamster lung) cells: the GIPR^{dn} bound GIP with normal affinity but failed to increase intracellular cAMP levels. Transgenic mice were then generated, expressing the mutated human GIPR cDNA under the control of the rat pro-insulin 2 gene promoter in pancreatic β-cells. These GIPR^{dn} transgenic mice demonstrated a disturbed development of the endocrine pancreas and showed severe diabetes mellitus (Herbach et al., 2005).

Diabetic nephropathy is one of the most feared diabetes-associated complications in humans but its pathogenesis is largely unknown. Analyzing the progression to advanced diabetic nephropathy is limited by the lack of appropriate animal models of advanced diabetic nephropathy. The mouse is particularly attractive for this sort of human disease modeling because of its tractability for genetic manipulation (Gurley et al., 2009). GIPR^{dn} transgenic mice have recently been shown to exhibit diabetes-associated kidney lesions that resemble early and intermediate stages of human diabetic kidney disease (Herbach et al., 2009). In addition, necropsy of a GIPR^{dn} transgenic mouse by coincidence revealed unilateral renal agenesia. The remaining

kidney of this animal showed advanced diabetes-associated glomerular and tubulo-interstital lesions that seemed more severe than kidney alterations of GIPR^{dn} transgenic animals investigated so far. This unintentional finding evoked the question if these severe and advanced kidney alterations would be reproducible by performing unilateral uninephrectomy early in life in these transgenic mice (Wanke and Herbach, personal communication).

The aim of the present study was to characterize clinical and pathomorphological effects of uninephrectomy on diabetes-associated kidney lesions of GIPR^{dn} transgenic diabetic mice. It was hypothesized, according to the unique renal findings in the one GIPR^{dn} transgenic mouse exhibiting unilateral renal agenesia, that uninephrectomy would aggravate the development of diabetic nephropathy in six- and twelve-month-old GIPR^{dn} transgenic mice, vs. sham operated transgenic and wild-type control mice. *Nagata et al*. showed in 1992 that uninephrectomy in young rats results in a higher incidence of glomerulosclerosis than in adults. The reason for this higher susceptibility in young animals is not fully understood, but this does suggest that uninephrectomy in young animals may represent a particularly promising model in which to study the development of advanced nephropathy (Nagata et al., 1992). Therefore, uninephrectomy was undertaken in 1-month-old male GIPR^{dn} transgenic diabetic mice.

In vivo findings

At 21 days of age, blood glucose levels were significantly elevated in transgenic animals and there was no difference in glucose concentrations between transgenic groups that were chosen for future uninephrectomy or sham operation. The finding of early onset diabetes is in line with the results of Herbach et al. (2005) who found the onset of diabetes mellitus in GIPR^{dn} transgenic mice to occur with the beginning intake of rodent chow, between 14 and 21 days of age (Herbach et al., 2005). The diabetic phenotype was further affirmed in the present study by measurement of serum glucose levels of four-, six-, and twelve-month-old mice. Serum glucose levels of transgenic mice were largely higher than those of wild-type mice, irrespective of the age at sampling. Uninephrectomy had no influence on serum glucose concentrations of either transgenic or wild-type mice, suggesting that a reduction of renal mass, i.e. uninephrectomy, has no effect on the diabetic state itself. This

observation is in line with findings in other diabetic remnant kidney models, e.g. the *db/db* mouse (Ninichuk et al., 2007).

Starting at about 2 months of age, the body weight of diabetic GIPR^{dn} transgenic animals was significantly lower than that of control mice. This finding is in coincidence with previous studies, using GIPR^{dn} transgenic mice (Herbach et al., 2005, Herbach et al., 2008). It was shown recently, that the reduced body weight of the transgenic animals was mainly due to the reduction of the weight of skin, carcass and abdominal fatty tissue, changes that were suggested to result from absolute insulin deficiency and disturbed lipogenesis (Herbach 2002, Herbach et al., 2008). This finding is in contrast to the situation in human diabetes mellitus, where accumulation of fat in the abdomen is a typical finding. Abdominal visceral fat is thought to be involved in glucose regulation and to potentiate the development of diabetes more than does subcutaneous fat (Resnick and Howard 2004).
Uninephrectomy had no influence on body-weights of either transgenic or control mice.

In humans, considerable evidence of the increased prevalence of hypertension in diabetic persons suggests that these two common chronic diseases frequently coexist, adding significantly to each others overall morbidity and mortality (Sowers et al., 2001). Therefore, blood pressure was determined non-invasively at 2 and 6 months of age. Both the systolic and diastolic blood pressure did not differ between the groups irrespective of the age investigated. Also, uninephrectomy had no influence on blood pressure of transgenic or wild-type control mice. Our results are in contrast to the findings in human patients suffering from diabetic nephropathy, which frequently exhibit hypertension. Hypertension is about twice as frequent in individuals with diabetes as in those without. Diabetes mellitus and hypertension are interrelated diseases that strongly predispose an individual to atherosclerotic cardiovascular disease. In 2003–2004, 75% of adult diabetic patients exhibited blood pressure greater than or equal to 130/80 mmHg, or used prescription medications for hypertension (ADA 2007). Diabetic nephropathy is an important contributing factor to the development of hypertension in the diabetic individual. The high blood pressure associated with diabetic nephropathy is usually characterized by sodium and fluid retention and increased peripheral vascular resistance (Sowers and Epstein 1995).

Other studies, using experimental animals, e.g. streptozotocin-, diet-induced or genetically altered diabetic mice (Breyer et al., 2005), however, do not develop hypertension, which is in line with results from the present study. Blood pressure tends to be reduced in most strains of streptozotocin-treated or diet-induced diabetic mice when significant hyperglycemia is present. Blood pressure does not seem to be dramatically affected by diabetes in genetically altered mice that are treated with streptozotocin, either (Breyer et al., 2005, Gurley et al., 2009). The explanation of this difference in blood pressure between diabetic mice and men remains a matter of debate. A recent study revealed that some rodent models are resistant to arteriosclerotic changes in coronary artery and spontaneous ischemia, which exist in many humans with diabetes mellitus (Kawada et al., 2010). In another recent study, researchers demonstrated that mice missing the gene „Junb“ which regulates arterial contraction capacity, cellular contractility, and motility, don't become hypertensive (Licht et al., 2010).

Serum parameters determined in the present study included important markers for renal lesions (urea, creatinine, albumin, total protein) and metabolism (glucose (discussed above), triglycerides). Serum urea and creatinine were both elevated in uninephrectomized and sham operated $GIPR^{dn}$ transgenic mice. This azotemia was not associated with clinical signs of renal failure and may therefore be due to severe diabetes-associated polyuria, resulting in sodium-chloride loss and dehydration, leading to the so-called hyponatremic syndrome/ chloropenic azotemia (Hepp and Häring 1999). Further, an increase in hepatic proteolysis due to insulin deficiency results in an increase of urea synthesis and may thereby increase serum urea levels (Hepp and Häring 1999, Janka et al., 1999). Another reason for the occurrence of azotemia in $GIPR^{dn}$ transgenic mice could be the decreased glomerular filtration due to advanced kidney changes and therefore, compensated retention of urinary excreted substances. In this study, the GFR of uninephrectomized and sham operated transgenic mice was actually reduced and the ACR was increased vs. the respective wild-type mice, therefore, diabetic kidney disease may contribute to azotemia in $GIPR^{dn}$ transgenic mice.

The slightly to significantly reduced total protein and albumin serum levels of transgenic animals may result from protein catabolism and/ or renal loss of proteins (Hepp and Häring 1999). Once GFR markedly decreases, the selectivity of

proteinuria disappears and both albumin and other macro-proteins appear in the urine in excessive amounts (Reddi and Camerini-Davalos 1990). It could be shown in this study, that the GFR is reduced and the ACR is increased in transgenic vs. wild-type mice, therefore, renal loss of proteins may be responsible for the reduced total protein and albumin serum levels. However, the reduced serum protein levels may also be secondary to insulin deficient diabetes mellitus of $GIPR^{dn}$ transgenic mice. Glucose uptake in muscles is insulin dependent and therefore reduced in insulin-deficient diabetes. Further, the amino acid uptake and protein synthesis is disturbed and proteolysis increased. Despite increased supply of free fatty acids, the insulin deficiency results in a catabolism of muscular tissue.

The glomerular filtration rate (GFR) is an important parameter for kidney function. At time of diagnosis of diabetes mellitus, human patients usually show renal hyperfunction and an increased GFR. With onset of microalbuminuria, the GFR returns to normal and when macroalbuminuria (albumin excretion more than 10-fold increased) is present, the GFR starts to decrease progressively (Mogensen et al., 1995). Both uninephrectomized and sham operated $GIPR^{dn}$ transgenic mice showed a reduced GFR and macroalbuminuria (see below). Uninephrectomy in transgenic mice led to a significantly lower GFR than sham operation and a significantly higher ACR. In wild-type mice, uninephrectomy did not influence the GFR or ACR. These findings suggest that glomerular injury, that accompanies the development of clinical nephropathy, is largely responsible for the reduction in GFR of transgenic mice (Marshall 2005). This is in agreement with previous studies in which total GFR in uninephrectomized male Sprague-Dawley rats was significantly lower than total GFR in sham-operated animals at 3 to 6 months after surgery (Nagata et al., 1992). Similar results were achieved in male Wistar rats that underwent 5/6 nephrectomy, a model of chronic renal failure, where the GFR of these subtotally nephrectomized rats was significantly lower than the GFR of control rats (Sviglerova et al., 2010). In contrast, the GFR in Akita diabetic mice was significantly increased compared with their respective non-diabetic, wild-type controls (Gurley et al., 2009), as observed in the stage of renal hyperfunction in human diabetic subjects (Mogensen et al., 1995).
It has to be mentioned that the GFR calculated in this study has to be interpreted carefully, since the Jaffé method was used to determine serum creatinine. New methods to accurately measure plasma creatinine by high performance liquid

chromatography (HPLC) have been established and have confirmed significant overestimation of plasma creatinine using Jaffé alkaline picrate-based methods. In mice with normal renal function, the picric acid–based method routinely overestimates HPLC-determined serum creatinine by two- to fivefold. When compared with inulin clearance, creatinine clearance determinations, using the Jaffé reaction underestimates GFR by >50% (Breyer et al., 2005). However, it has not been analyzed whether diabetes in mice influences serum creatinine results determined by Jaffé method. In humans, ketoacidosis is known to influence serum creatinine, using Jaffé method but since GIPR^{dn} transgenic mice do not show ketoacidosis, it is likely that serum creatinine levels of both transgenic and wild-type mice in this study were overestimated by approximately the same degree (Brosius et al., 2009).

Urine analyses were performed to further analyze renal function and clinical features of kidney disease. Urinary creatinine levels of transgenic mice were significantly lower than those of wild-type mice, shortly after diabetes onset, which is a common finding in uncontrolled diabetes, e.g. in GIPR^{dn} transgenic mice (Herbach et al., 2009). Uninephrectomy did not influence this parameter in either transgenic or wild-type mice. Both uninephrectomized and sham operated GIPR^{dn} transgenic mice, exhibited a higher ACR as well as higher ACR in 24 hour urine samples than their corresponding wild-type control mice. The ACR in spot urine samples of sham operated transgenic mice was increased up to 3-fold, whereas that of uninephrectomized transgenic mice was increased up to 92-fold vs. the respective wild-type controls. The ACR in 24 hour urine samples of sham operated transgenic mice was increased 73-fold, that of uninephrectomized transgenic mice was increased 400-fold vs. the respective wild-type controls, which, with regard to the staging in humans (Mogensen et al., 1995), indicates macroalbuminuria/insipient nephropathy in GIPR^{dn} transgenic mice,. According to Breyer et al., a 10-fold increase in the ACR may be regarded as abnormal albuminuria and an increase in the ACR between 100-1000-fold was suggested to reflect established diabetic renal disease in diabetic mouse models (Breyer et al., 2005). Therefore, both uninephrectomized and sham operated GIPR^{dn} transgenic mice show clinical signs of diabetic kidney disease. Comparable large increases in albuminuria were rarely observed in studies using diabetic mice. In the KK-Ay mouse fed a high-cholesterol diet, a 1000-fold increased albuminuria was suggested, but not in the Akita mouse

bearing an *Ins2*^{C96Y} mutation or the diabetic eNOS knockout mouse (Breyer et al., 2005, Gurley et al., 2009, Mohan et al., 2008). However, the NONcNZO mouse develops significant and progressively increasing albuminuria, with urine albumin-creatinine ratios >1000µg/mg after 1 year of age (Brosius et al., 2009). Additionally, uninephrectomy vs. sham operation in GIPR^{dn} transgenic mice provoked an about 10-fold increased ACR in both spot urine and 24 hour urine samples. In contrast, the ACR of spot urine samples and the ACR in 24 hour urine samples of uninephrectomized wild-type mice was unchanged vs. sham operated wild-type mice.

In summary, the clinical results, including increased serum concentrations of creatinine and urea, decreased urinary creatinine and GFR, and higher ACR of GIPR^{dn} transgenic mice, are the typical biochemical signs of chronic kidney disease (Sviglerova et al., 2010). In respect of these findings it can be suggested, that uninephrectomy in GIPR^{dn} transgenic mice aggravates the onset and severity of kidney damage.

Morphological findings

Functional markers of chronic renal failure were associated with morphological changes in the remnant kidney in studies, using 5/6 nephrectomized Wistar male rats (Sviglerova et al., 2010). Since the ACR and GFR of uninephrectomized GIPR^{dn} transgenic mice was higher than that of sham operated transgenic animals, the development of aggravated kidney lesions was expected in uninephrectomized vs. sham operated GIPR^{dn} transgenic mice.

At six months of age, both uninephrectomized and sham operated GIPR^{dn} transgenic mice, exhibited a greater kidney volume than the respective wild-type animals. Renal hypertrophy generally is a characteristic change in early stages of human diabetes (Schwieger and Fine 1990) and various rodent models of diabetes, e.g. GIPR^{dn} transgenic mice (Herbach et al., 2009), the BTBR *ob/ob* mouse, the KK-A^{y} mouse and the NONcNZO mouse, and streptozozocin diabetic mice and rats (Brosius et al., 2009, Kakoki et al., 2004, Rees and Alcolado 2005). Studies in animals revealed that this renal enlargement is mostly due to a combination of tubular hypertrophy and hyperplasia and interstitial expansion (Bilous 2001).

Both GIPR^{dn} transgenic and wild-type mice that were uninephrectomized exhibited increased kidney volumes as compared to their sham operated counterparts. Compensatory renal growth is an adaptive response to the loss of renal mass, as shown in studies, using uninephrectomized Wistar rats, Sprague-Dawley rats, and C57Bl/6 mice, which exhibited increased kidney volumes as compared to their sham operated counterparts (Liu and Preisig 2002, Okada et al., 2010, Sviglerova et al., 2010).

The kidney volumes of 12-month-old uninephrectomized wild-type mice were significantly higher than those of age-matched sham operated controls. However, there were no differences in the kidney volumes of transgenic mice as opposed to controls or between the transgenic uninephrectomized and sham operated groups at 12 months of age. According to a study in uninephrectomized rats, persistent proteinuria causes apoptosis in tubular cells. Apoptosis (programmed cell death) is a gene-regulated process that is recognized to play an important role in maintaining cell number homeostasis both in health and disease. Unregulated excessive apoptosis can contribute to renal damage by depletion of glomerular and tubulointerstitial cells, characteristic of progressive chronic nephropathies (Tejera et al., 2004). Since uninephrectomized GIPR^{dn} transgenic mice exhibited pronounced albuminuria, enhanced apoptosis might explain the lower kidney volumes of 12-month-old vs. 6-month-old transgenic mice. The findings in GIPR^{dn} transgenic mice are in coincidence with findings in human patients, where in early stages of diabetes mellitus, the kidneys are enlarged (Bilous 2001). However, later in the course of the disease in humans, small kidneys with a granular surface are frequently observed (Heptinstall 1991), a finding we could only demonstrate in one uninephrectomized GIPR^{dn} transgenic mouse at 7 months of age (see below).

Histologically, the glomeruli of uninephrectomized and sham operated GIPR^{dn} transgenic mice at six and twelve months of age showed mesangial expansion, focal segmental, sometimes panglomerular glomerulosclerosis, adhesions between the glomerular tuft and the capsule of Bowman, and large distorted capillaries. Tubulointerstitial lesions of transgenic mice included protein reabsorption droplets in proximal tubular epithelia, proteinaceous casts in distal tubules, focal tubular atrophy and few focal interstitial mononuclear inflammatory cell-infiltrates. These findings are

in coincidence with observations in a previous study, where glomerular damage was prominent in GIPR^{dn} transgenic mice, including advanced glomerulosclerosis, tubulointerstitial lesions and proteinuria (Herbach et al., 2009). Early uninephrectomy aggravated the development of glomerular and tubulo-interstitial lesions in transgenic mice of the present study vs. sham operated animals in an age-related manner (e.g. diffuse segmental and frequently also panglomerular glomerulosclerosis was evident), consistent with the histopathological abnormalities of advanced diabetic nephropathy in humans. These pathological changes seen in the human diabetic kidney at an advanced point of disease are tubular loss accompanied by glomerular and vascular sclerosis. The tubules undergoing atrophy show thickened basement membranes. The interstitial tissue is fibrotic and contains inflammatory cells (Heptinstall 1991, Tervaert et al., 2010). A previous study in db/db mice showed that global glomerulosclerosis at 6 months of age was more common in uninephrectomized vs. sham operated db/db mice, where only minor glomerular changes were observed. Additionally, early uninephrectomy significantly enhanced all markers of tubulo-interstitial injury as compared to sham-operated db/db mice (Ninichuk et al., 2007).

One uninephrectomised GIPR^{dn} transgenic mouse was euthanized at 7 months of age due to reduced general condition, loss of body weight and signs of anemia. The remnant kidney was smaller than that of all other transgenic animals and exhibited a granular surface, indicating chronic nephropathy. Glomerulosclerotic lesions were evident in a diffuse panglomerular manner and this animal exhibited cystic dilation of many tubules, hyaline casts in distal tubules, tubular atrophy, vast interstitial fibrosis and focal mononuclear cell infiltration. The macroscopic and histologic appearance of the kidney of this 7-month-old animal led to the diagnosis of end-stage renal disease. This is the first observation of terminal renal failure in a mouse model of diabetic kidney disease.

Glomerular changes due to diabetes or uninephrectomy were investigated, using quantitative stereological methods in GIPR^{dn} transgenic and wild-type mice. The mean glomerular volume was significantly increased in 6-month-old uninephrectomized and sham operated transgenic mice vs. controls. This finding is in coincidence with previous observations in GIPR^{dn} transgenic mice (Herbach et al., 2009). Up to 8 weeks of age, the mean glomerular volume of male transgenic mice

was not yet increased vs. male controls. After that, a progressive increase in the mean glomerular volume was observed in both male and female transgenic mice (Herbach et al., 2009). Glomerular hypertrophy is observed in various diabetic animal models. By 18–20 months of age, glomerular enlargement and mesangial matrix expansion become obvious in the db/db mouse (Sharma et al., 2003), the BTBR ob/ob mouse (Hudkins et al., 2010), and streptozotocin-induced diabetic mice (Mizuno et al., 2004). The current investigation also showed a significant increase in the mean glomerular volume of uninephrectomized compared to sham operated GIPR^{dn} transgenic as well as uninephrectomized vs. sham operated wild-type mice at 6 months of age. Glomeruli of uninephrectomized wild-type and sham operated transgenic animals showed an equal mean glomerular volume, showing that uninephrectomy in healthy animals leads to the same extent of glomerular hypertrophy as hyperglycemia. In a remnant kidney mouse model (5/6 nephrectomy) without diabetes, a 40% increase in glomerular tuft area was observed vs. sham operated mice (Nakayama et al., 2009), a similar increase as of the mean glomerular area of GIPR^{dn} transgenic diabetic vs. non-diabetic control animals (data not shown). Uninephrectomy in young male Sprague-Dawley rats also caused increased glomerular tuft growth compared to sham operated controls. Along with the hypertrophic growth of glomeruli in uninephrectomized rats, several kinds of structural changes were observed increasing in frequency and severity with time. These uninephrectomy enforced alterations in the Sprague-Dawley rat are seen in changes in the width and shape of glomerular capillaries associated with changes in the distribution of the associated mesangium, in various changes in the podocyte structure; and in tuft adhesions to Bowman's capsule (Nagata and Kriz 1992), similar changes that were observed in GIPR^{dn} transgenic mice investigated the present study.

As a consequence of glomerular hypertrophy, the mean glomerular mesangium and capillary volumes were significantly increased in both uninephrectomized and sham operated GIPR^{dn} transgenic mice vs. controls, despite unchanged volume fractions of mesangium and capillaries.

The mean glomerular mesangium and capillary volumes increased significantly in both uninephrectomized wild-type and transgenic animals from 1 to 6 months of age, but this increase was more pronounced in uninephrectomized transgenic mice.

The most characteristic and clinically important glomerular lesion in human diabetes mellitus is mesangial expansion. The mesangial volume fraction ($Vv_{(mes/glom)}$) was the main structural predictor of the rate of decline in GFR and albuminuria, whereby a large $Vv_{(mes/glom)}$ was associated with increased albuminuria and loss in GFR (Christensen et al., 2001). In a study by Østerby et al. (1993) in humans, the renal lesions were examined, using a glomerulopathy index, combining the basement membrane thickness and $Vv_{(mes/glom)}$. It was shown that there is a relationship between the course of kidney function and the glomerulopathy index (Osterby et al., 1993). A pathophysiological study also demonstrated that the relationship between $Vv_{(mes/glom)}$ and rate of decline in GFR in human patients probably results from the expanding mesangium, compromising the structure of glomerular capillaries and reducing the ultrafiltration coefficient filtration (defined as the product of effective hydraulic permeability and total glomerular capillary surface area of the kidney) (Christensen et al., 2001). Mesangial matrix fraction increases are frequently found in diabetic animals, such as db/db, BTBR ob/ob, and streptozotocin treated mice and also rats vs. non-diabetic controls (Chen et al., 2003, Hudkins et al., 2010, Melhem et al., 2002, Mizuno et al., 2004).

The numerical volume density of podocytes in glomeruli of 6-month-old transgenic mice was significantly lower than that of the respective wild-type mice. This finding is in line with a previous study, where the numerical volume density of podocytes in glomeruli was significantly reduced in both 8-week-old male and female $GIPR^{dn}$ transgenic mice (Herbach et al., 2009). Della Vestra et al. suggested that the numerical volume density of podocytes is functionally more relevant than absolute numbers in type 2 diabetic patients, since the numerical volume density of podocytes but not absolute numbers is inversely related to albumin excretion rate. Podocytes in enlarged glomeruli have to cover a larger glomerular basement membrane area and are subjected to increased mechanical stress and injury. Widening of foot processes and increased albumin excretion, loss of podocytes and glomerulosclerosis are the consequences (Dalla Vestra *et al.*, 2003). However, in the present study only the mean glomerular volume (and consequently the mean mesangial and capillary volumes) was altered significantly more in uninephrectomized than in sham operated transgenic mice but the numerical volume density of podocytes was equal despite large difference in the ACR in spot urine samples. It therefore seems likely that the

numerical volume density of podocytes may not be a good predictor for severity of albuminuria in GIPR^{dn} transgenic mice.

The number of podocytes was not altered in GIPR^{dn} transgenic mice analyzed in the present and a previous study (Herbach et al., 2009). In a different study in OVE26 diabetic mice, Teiken et al. (2007) documented a substantial reduction of the mean podocyte number per glomerulus between 150 days and 450 days of age, suggesting that podocyte loss could also be an age-related matter (Teiken et al., 2008). In diabetic ob/ob mice on the black and tan, brachyuric genetic background (BTBR ob/ob mice), the number of podocytes was stated to be reduced early in the disease course vs. wild-type mice and a loss of podocytes was postulated. However, the number of podocytes per glomerulus was not determined using state of the art quantitative-stereological techniques, and in addition, podocyte number of 8- and 20-week old BTBR ob/ob mice was essentially the same, arguing against podocyte loss. Further, there was no increase in the number of apoptotic podocytes in the BTBR ob/ob mice at either early or late time points compared with wild-type littermates (Hudkins et al., 2010). The podocyte density, however, was significantly reduced in BTBR ob/ob mice compared with BTBR WT mice at every time point studied and this diminished podocyte density occurred in conjunction with increased glomerular volumes in BTBR ob/ob vs. BTBR WT mice (Hudkins et al., 2010), similar to GIPR^{dn} transgenic mice. Likewise, in male Sprague-Dawley rats, the average number of podocytes per glomerulus changed neither in control animals, nor after uninephrectomy. Due to the increase in tuft volume and the unaltered podocyte number, the numerical density of podocytes decreased with age in both groups. The lowest values were found in the hypertrophied glomeruli of the uninephrectomized group. This study in the remnant kidney rat could show that the elaborately shaped podocyte is incapable of replication. Remaining podocytes are obliged to grow and to extend their foot processes to maintain the area covered (Nagata and Kriz 1992). Wanke et al. (2001) demonstrated that podocyte hypertrophy is correlated with increasing glomerular volume, leading to severe podocyte stretching, due to the podocytes' inability to proliferate, resulting in detachment of podocytes. These podocyte alterations in the growth hormone (GH) transgenic mouse (TM) provide evidence that podocyte damage plays a significant role in the pathogenesis of progressive nephropathy (Wanke et al., 2001). A loss of podocytes in patients with

clinical nephropathy was associated with an increase in the surface area covered by each remaining cell and was also accompanied by increases in the volumes of remaining podocytes. These findings suggested that podocyte loss contributes to the progression of diabetic nephropathy and that these morphological changes may relate to the loss of glomerular permselectivity in diabetic nephropathy (Pagtalunan et al., 1997). Another study in human patients with diabetic nephropathy showed that podocyte loss is correlated with clinical and pathological disease progression (e.g. proteinuria and mesangial expansion). Podocyte loss was suggested to show a stronger relationship with the renal prognosis than glomerular basement membrane thickening or mesangial expansion (Mundel and Shankland 2002). In the present study neither uninephrectomised nor sham operated GIPR^{dn} transgenic mice showed reduced numbers of podocytes vs. wild-type mice, despite marked albuminuria, therefore, the number of podocytes does not seem to be related to the development of albuminuria in GIPR^{dn} transgenic mice.

At 6 months of age, transgenic mice exhibited a significantly higher mean podocyte volume (podocyte hypertrophy) vs. the respective control mice. This finding is in coincidence with a previous study where it was shown that in male GIPR^{dn} transgenic mice, podocyte hypertrophy occurred even before glomerular hypertrophy was evident, and without changes in blood pressure (Herbach et al., 2009). Therefore, it was concluded that hyperglycemia directly influenced glomerular epithelial cell growth in early disease stages in GIPR^{dn} transgenic mice. Adaptive growth of the podocytes due to glomerular hypertrophy (Wiggins *et al.*, 2005) may further contribute to podocyte growth in later stages of the disease, as analyzed in the present study. However, in 6-month-old uninephrectomized wild-type mice, the podocyte volume was only slightly but not significantly higher than that of sham operated controls, despite significantly higher mean glomerular volume, and the mean podocyte volume of sham operated transgenic mice was significantly higher than that of uninephrectomized wild-type mice despite equal mean glomerular volumes. In addition, podocytes of both sham operated and uninephrectomized transgenic mice were equally sized, although the mean glomerular volumes were significantly different. All these observations argue for a more pronounced impact of hyperglycemia on podocyte growth than adaptive growth.

Hypertrophy of renal cells is thought to contribute to diabetes associated kidney lesions, such as glomerulosclerosis, tubular atrophy and interstitial fibrosis, which was also observed in the present study. Podocyte hypertrophy, caused by high glucose concentrations, may eventually lead to podocyte loss and glomerulosclerosis (Gross et al., 2003, Kim 2005).

Reduction of renal mass does not uniformly accelerate the progression of kidney disease in humans or mice (Zeier et al., 1992) However, a reduction of renal mass can particularly accelerate the progression of glomerulopathies probably by enhancing glomerular hyperfiltration (Ritz 2006). Uninephrectomy may be a preferred method of accelerating diabetic nephropathy in $GIPR^{dn}$ transgenic mice because it does not affect unrelated or other pathomechanisms of diabetic nephropathy. Our data shows that e.g. body weight, blood and serum glucose concentrations, urine creatinine, ACR, GFR and mean glomerular capillary volume were not affected by surgery in wild-type mice. The remnant kidneys of early uninephrectomized $GIPR^{dn}$ transgenic diabetic mice resemble the changes seen in humans with diabetic kidney disease. This model shows a high degree of reproducibility with a minimum of undesirable side-effects. Thus, uninephrectomized $GIPR^{dn}$ transgenic mice represent a useful tool in the study of advanced diabetes-associated kidney changes.
Together, we conclude that uninephrectomy performed at 4 weeks of age aggravates the development of diabetes-associated kidney lesions in male $GIPR^{dn}$ transgenic mice. This model may be instrumental for validating targets potentially involved in the progression of diabetic renal disease.

6. Summary

Clinical and pathomorphological characterization of uninephrectomized GIPR^{dn} transgenic diabetic mice

Diabetic nephropathy is one of the leading causes of end-stage renal disease in humans, however, the pathogenesis of this feared diabetes-associated complication is far from being understood. Diabetic animal models are used to study the pathogenesis of diabetic nephropathy but the existing experimental animals develop kidney lesions that closely resemble those observed in human patients only in the early stages. The aim of this study was to analyze whether uninephrectomy is capable of aggravating the diabetes-associated kidney lesions in GIPR^{dn} transgenic mice, a novel animal model for diabetic renal disease.

GIPR^{dn} transgenic and wild-type control mice either underwent uninephrectomy or sham operation at 1 month of age. *In vivo* investigations included the determination of body weights, blood pressure, blood glucose, serum urea, creatinine, total protein, albumin, triglyceride, and chloride levels. The urine albumin and creatinine concentrations were determined in regularly taken spot urine samples and the albumin to creatinine ratio (ACR) was calculated. The ACR in 24 hour urine samples as well as the glomerular filtration rate (GFR) were calculated at 4 months of age. Histological and quantitative stereological analyses of the kidneys were performed, using 6- and 12-month-old animals. The mean glomerular volume, mean glomerular mesangium and capillary volume, the numerical volume density of podocytes in glomeruli, and the number and mean size of podocytes were estimated.

At weaning (21 days), all transgenic animals already exhibited severe hyperglycemia and from 2 months of age onwards, transgenic mice weighed less than wild-type mice. Uninephrectomy did not influence blood glucose or body weights of either GIPR^{dn} transgenic or wild-type mice vs. sham operated animals. Neither diabetes nor uninephrectomy had an impact on blood pressure in the examined groups. Between one and two months of age, GIPR^{dn} transgenic mice showed reduced urine creatinine levels, and from 2 months of age onwards, their ACR was significantly increased vs. wild-type mice. Uninephrectomy had no influence on urine creatinine, ACR and GFR of wild-type mice vs. sham operated wild-types. In transgenic mice, urine creatinine was also not influenced by uninephrectomy, but the ACR was

significantly higher and GFR was significantly lower in uninephrectomized than in sham operated transgenic mice.

Histologically, glomeruli of transgenic mice showed focal segmental to panglomerular glomerulosclerosis, synechia between the glomerular tuft and the capsule of Bowman, and large distorted capillaries. Tubulo-interstitial lesions of transgenic mice included tubular atrophy, proteinaceous casts in distal tubules, focal interstitial fibrosis and mononuclear cell infiltration. The severity of these renal lesions progressed in an age-related manner and was enhanced by uninephrectomy in transgenic mice. One uninephrectomized transgenic animal exhibited renal features of end-stage kidney disease at 7 months of age. Wild-type mice occasionally showed mild kidney lesions, which also deteriorated slightly in an age-related manner but were never as pronounced as in transgenic animals. The kidney volume, mean glomerular volume and mean glomerular mesangium volume of 6-month-old transgenic mice was significantly increased vs. wild-type mice and uninephrectomy led to significantly enhanced kidney and glomerular growth, as well as mesangial expansion in both transgenic and wild-type mice vs. their sham operated counter parts.

The numerical volume density of podocytes was significantly decreased and the mean podocyte volume was significantly increased in transgenic vs. wild-type mice. Uninephrectomy did not influence these two parameters of either transgenic or wild-type mice vs. their sham operated counterparts.

In summary, early uninephrectomy aggravates clinical and pathomorphological features of chronic renal disease in GIPR^{dn} transgenic mice. Therefore, uninephrectomized GIPR^{dn} transgenic mice provide a valuable new model for studying the pathogenesis of diabetic kidney disease and for testing novel treatment strategies.

7. Zusammenfassung

Klinische und pathomorphologische Charakterisierung unilateral nephrektomierter GIPR^{dn} transgener diabetischer Mäuse

Die diabetische Nephropathie ist eine der Hauptursachen des chronischen Nierenversagens des Menschen, wobei die Pathogenese dieser gefürchteten Diabetes-assoziierten Komplikation bei weitem nicht erforscht ist. Diabetische

Tiermodelle werden eingesetzt, um die Pathogenese der diabetischen Nephropathie zu untersuchen, jedoch gleichen die Nierenschäden bei den vorhandenen Versuchstieren jenen bei humanen Patienten nur in den Frühstadien. Das Ziel dieser Studie war es zu untersuchen, ob durch Uninephrektomie die Diabetes-assoziierten Nierenveränderungen bei $GIPR^{dn}$ transgenen Mäusen, einem neuartigen Tiermodell für diabetische Nephropathie, verstärkt werden können.

$GIPR^{dn}$ transgene Mäuse und Wildtypmäuse wurden im Alter von 1 Monat entweder uninephrektomiert oder scheinoperiert. *In vivo* Untersuchungen beinhalteten die Bestimmung von Körpergewicht, Blutdruck, Blutzucker und die Messung der Harnstoff-, Kreatinin-, Gesamtprotein-, Albumin-, Triglyzerid- und Chloridkonzentration im Serum. In regelmäßig genommenen Spontanurinproben wurden Albumin- und Kreatininkonzentrationen gemessen und das Albumin-Kreatinin-Verhältnis (ACR) berechnet. Die ACR in den 24 Stunden Sammelharnproben sowie die glomeruläre Filtrationsrate (GFR) wurden im Alter von 4 Monaten bestimmt. Histologische und quantitativ-stereologische Analysen der Nieren wurden bei 6- und 12-Monate alten Tieren durchgeführt. Das mittlere Glomerulumvolumen, das mittlere glomeruläre Mesangium- und Kapillarvolumen, die numerische Volumendichte der Podozyten in den Glomerula, sowie Anzahl und mittlere Größe der Podozyten wurden analysiert.

Beim Absetzen (21 Tage) zeigten alle transgenen Tiere bereits eine schwere Hyperglykämie und ab einem Alter von 2 Monaten wogen transgene Mäuse weniger als Wildtypmäuse. Die Uninephrektomie hatte keinen Einfluss auf die Blutzuckerkonzentration oder das Körpergewicht bei $GIPR^{dn}$ transgenen oder Wildtyp Mäusen im Vergleich zu Werten bei scheinoperierten Tieren. Weder der Diabetes noch die Uninephrektomie wirkten sich auf den Blutdruck in den verschiedenen Mäusegruppen aus. Im Alter von ein bis zwei Monaten waren bei $GIPR^{dn}$ transgenen Mäusen die Harnkreatininwerte niedriger und ab einem Alter von 2 Monaten war ihre ACR signifikant höher als bei Wildtyp-Mäusen. Die Uninephrektomie hatte keinen Einfluss auf Harnkreatinin, ACR und GFR von Wildtypmäusen im Vergleich zu Werten bei scheinoperierten Wildtypen. Bei transgenen Mäusen wurde die Harnkreatininkonzentration ebenfalls nicht durch die Uninephrektomie beeinflusst, aber bei uninephrektomierten transgenen Mäusen war die ACR signifikant höher und die GFR signifikant niedriger als bei scheinoperierten transgenen Tieren.

Histologisch zeigten die Glomerula von transgenen Mäusen fokal segmentale und panglomeruläre Glomerulosklerose, Synechien zwischen dem Glomerulum und der Bowman'schen Kapsel und große dilatierte Kapillaren. Tubulointerstitielle Läsionen transgener Mäuse beinhalteten Tubulusatrophie, Proteinzylinder in distalen Tubuli, fokale interstitielle Fibrose und mononukleäre Zellinfiltrate. Der Schweregrad der Nierenschädigung schritt altersabhängig voran und wurde durch die Uninephrektomie bei transgenen Mäusen verstärkt. Ein 7 Monate altes uninephrektomiertes transgenes Tier zeigte renale Veränderungen im Sinne einer terminalen Nephropathie. Wildtypmäuse wiesen nur gelegentlich geringgradige Nierenveränderungen auf, die altersassoziiert leicht zunahmen, jedoch bei weitem nicht dem Grad der Veränderungen bei transgenen Tieren entsprachen.

Das Nierenvolumen, das mittlere Glomerulumvolumen und das mittlere glomeruläre Mesangiumvolumen 6 Monate alter transgener Mäuse war im Vergleich zu Wildtypmäusen signifikant erhöht und durch die Uninephrektomie stieg das renale und glomeruläre Wachstum bei transgenen Tieren noch einmal erheblich im Vergleich zu scheinoperierten $GIPR^{dn}$ transgenen Mäusen. Ferner führte die Uninephrektomie sowohl bei transgenen als auch Wildtypmäusen zur Zunahme des mittleren glomerulären Mesangiumvolumens gegenüber entsprechenden scheinoperierten Tieren.

Bei den transgenen Mäusen war die numerische Volumendichte der Podozyten in Glomerula deutlich verringert und das mittlere Podozytenvolumen signifikant erhöht gegenüber Wildtypmäusen. Die Uninephrektomie hatte weder bei transgenen noch bei Wildtyp-Mäusen einen Einfluss auf diese beiden Parameter gegenüber den scheinoperierten Pendants.

Zusammenfassend zeigt die vorliegende Studie, dass die frühzeitige Uninephrektomie das klinische und pathomorphologische Erscheinungsbild der chronischen Nierenerkrankung bei $GIPR^{dn}$ transgenen Mäusen verstärkt. Uninephrektomierte $GIPR^{dn}$ transgene Mäuse bieten daher ein wertvolles neuartiges Modell für das Studium der Pathogenese der diabetischen Nierenerkrankung sowie zur Erprobung von neuartigen Behandlungsstrategien.

8. References

ADA (2007) American Diabetes Association National Diabetes Fact Sheet. Diabetes Statistics, Available from http://www.diabetes.org/

Baggio L, Kieffer TJ, Drucker DJ (2000) Glucagon-like peptide-1, but not glucose-dependent insulinotropic peptide, regulates fasting glycemia and nonenteral glucose clearance in mice. Endocrinology 141: 3703-3709

Balwierz A, Polus A, Razny U, Wator L, Dyduch G, Tomaszewska R, Scherneck S, Joost H, Dembinska-Kiec A (2009) Angiogenesis in the New Zealand obese mouse model fed with high fat diet. Lipids Health Dis 8: 13

Bilous R (2001) Renal structural damage in IDDM and NIDDM-functional relationship. In: Hasslacher C (ed) Diabetic Nephropathy. John Wiley & Sons, Ltd, Chichester, UK

Breyer MD, Bottinger E, Brosius FC, 3rd, Coffman TM, Harris RC, Heilig CW, Sharma K (2005) Mouse models of diabetic nephropathy. J Am Soc Nephrol 16: 27-45

Brosius FC, 3rd, Alpers CE, Bottinger EP, Breyer MD, Coffman TM, Gurley SB, Harris RC, Kakoki M, Kretzler M, Leiter EH, Levi M, McIndoe RA, Sharma K, Smithies O, Susztak K, Takahashi N, Takahashi T (2009) Mouse models of diabetic nephropathy. J Am Soc Nephrol 20: 2503-2512

Camici M (2005) Renal glomerular permselectivity and vascular endothelium. Biomed Pharmacother 59: 30-37

Caulfield JB (1957) Effects of varying the vehicle for OsO4 in tissue fixation. J Biophys Biochem Cytol 3: 827-830

Chanutin A, Ferris EB (1932) Experimental renal insufficiency produced by partial nephrectomy: I. Control Diet. Arch Intern Med 49: 767-787

Chen S, Iglesias-de la Cruz MC, Jim B, Hong SW, Isono M, Ziyadeh FN (2003) Reversibility of established diabetic glomerulopathy by anti-TGF-beta antibodies in db/db mice. Biochem Biophys Res Commun 300: 16-22

Christensen PK, Larsen S, Horn T, Olsen S, Parving HH (2001) Renal function and structure in albuminuric type 2 diabetic patients without retinopathy. Nephrol Dial Transplant 16: 2337-2347

Costa AF, Pereira Lde P, Ferreira ML, Silva PC, Chagar VL, Schanaider A (2009) [Surgical model of chronic renal failure: study in rabbits]. Rev Col Bras Cir 36: 78-84

Dalla Vestra M, Masiero A, Roiter AM, Saller A, Crepaldi G, Fioretto P (2003) Is podocyte injury relevant in diabetic nephropathy? Studies in patients with type 2 diabetes. Diabetes 52: 1031-1035

Daneshgari F, Leiter EH, Liu G, Reeder J (2009) Animal models of diabetic uropathy. J Urol 182: S8-13

Figueroa CD, Taberner PV (1994) Pancreatic islet hypertrophy in spontaneous maturity onset obese-diabetic CBA/Ca mice. Int J Biochem 26: 1299-1303

Frankel BJ, Gerich JE, Hagura R, Fanska RE, Gerritsen GC, Grodsky GM (1974) Abnormal secretion of insulin and glucagon by the in vitro perfused pancreas of the genetically diabetic Chinese hamster. J Clin Invest 53: 1637-1646

Gerritsen GC (1982) The Chinese hamster as a model for the study of diabetes mellitus. Diabetes 31: 14-23

Gomori G (1946) A new histochemical test for glycogen and mucin. Am J Clin Pathol 10: 177-179

Gross ML, El-Shakmak A, Szabo A, Koch A, Kuhlmann A, Munter K, Ritz E, Amann K (2003) ACE-inhibitors but not endothelin receptor blockers prevent podocyte loss in early diabetic nephropathy. Diabetologia 46: 856-868

Gurley SB, Mach CL, Stegbauer J, Yang J, Snow KP, Hu A, Meyer TW, Coffman TM (2009) Influence of genetic background on albuminuria and kidney injury in Ins2(+/C96Y) (Akita) mice. Am J Physiol Renal Physiol 298: F788-795

Hansotia T, Baggio LL, Tsukiyama K, Miyawaki K, Yamada Y, Thorens B, Seino Y, Drucker DJ (2002) Combined genetic disruption of incretin signaling produces abnormalities in glucose homeostasis and body weight in GLP-1R-/-:GIPR-/- double mutant mice. Diabetes 51: Suppl 2, A66

Hasslacher C, Wolf G, Kempe P, Ritz E (2009) Diabetische Nephropathie. Diabetologie 4: 127-130

Hepp KD, Häring HU (1999) Einführung in die Biochemie und Pathophysiologie des Stoffwechsels. In: Mehnert H, Standl E, Usadel KH (eds) Diabetologie in Klinik und Praxis. Georg Thieme Verlag, Stuttgart, Germany, pp 1-31

Heptinstall RH (1991) Diabetes mellitus and gout. Little, Brown and Company, Boston, Toronto

Herbach N (2002) Clinical and pathological characterization of a novel transgenic animal model of diabetes mellitus expressing a dominant negative glucosedependent insulinotropic polypeptide receptor (GIPRdn). Inaugural - Dissertation to achieve the doctor title of veterinary medicine at the Faculty of Veterinary Medicine of the Ludwig-Maximilian-University, Munich

Herbach N, Goeke B, Schneider M, Hermanns W, Wolf E, Wanke R (2005) Overexpression of a dominant negative GIP receptor in transgenic mice results in disturbed postnatal pancreatic islet and beta-cell development. Regul Pept 125: 103-117

Herbach N, Goke B, Wolf E, Wanke R (2008) Diets influence the diabetic phenotype of transgenic mice expressing a dominant negative glucose-dependent insulinotropic polypeptide receptor (GIPRdn). Regul Pept 146: 260-270

Herbach N, Schairer I, Blutke A, Kautz S, Siebert A, Goke B, Wolf E, Wanke R (2009) Diabetic kidney lesions of GIPRdn transgenic mice: podocyte hypertrophy and thickening of the GBM precede glomerular hypertrophy and glomerulosclerosis. Am J Physiol Renal Physiol 296: F819-829

Hermanns W, Liebig K, Schulz LC (1981) Postembedding immunohistochemical demonstration of antigen in experimental polyarthritis using plastic embedded whole joints. Histochemistry 73: 439-446

Hirose K, Osterby R, Nozawa M, Gundersen HJ (1982) Development of glomerular lesions in experimental long-term diabetes in the rat. Kidney Int 21: 689-695

Hudkins KL, Pichaiwong W, Wietecha T, Kowalewska J, Banas MC, Spencer MW, Muhlfeld A, Koelling M, Pippin JW, Shankland SJ, Askari B, Rabaglia ME, Keller MP, Attie AD, Alpers CE (2010) BTBR Ob/Ob mutant mice model progressive diabetic nephropathy. J Am Soc Nephrol 21: 1533-1542

IDF (2006) International Diabetes Federation. The Diabetes Atlas, Available from http://www.diabetesatlas.org/downloads

Ikeda H (1994) KK mouse. Diabetes Res Clin Pract 24 Suppl: S313-316

Janka H, Standl E, Standl R (1999) Allgemeiner Überblick über die Angiopathien. In: Mehnert H, Standl R, Usadel KH (eds) Diabetologie in Klinik und Praxis. Georg Thieme Verlag, Stuttgart, pp 334-372

Kakoki M, Takahashi N, Jennette JC, Smithies O (2004) Diabetic nephropathy is markedly enhanced in mice lacking the bradykinin B2 receptor. Proc Natl Acad Sci U S A 101: 13302-13305

Kawada T, Miyata S, Shimada T, Sanzen Y, Ito M, Hemmi C, Iizuka S, Suzuki W, Mihara K, Aburada M, Nakazawa M (2010) A study of cardiovascular function in Tsumura Suzuki obese diabetes, a new model mouse of type 2 diabetes. Biol Pharm Bull 33: 998-1003

Kawano K, Hirashima T, Mori S, Natori T (1994) OLETF (Otsuka Long-Evans Tokushima Fatty) rat: a new NIDDM rat strain. Diabetes Res Clin Pract 24 Suppl: S317-320

Kempe HP, Engelmann K, Gretz N, Hasslacher C (1993) Models of Diabetes for Studying Diabetic Nephropathy. Karger, Basel

Kerner W (1998) Klassifikation und Diagnose des Diabetes mellitus. Dt Ärztebl 95: A3144-3148

Kerner W, Brückel J, Böhm BO (2004) Definition, Klassifikation und Diagnostik des Diabetes mellitus. Evidenzbasierte Leitlinie der Deutschen Diabetes-Gesellschaft,

Available from http://www.deutsche-diabetes-gesellschaft.de/leitlinien/EBL_Klassifikation_Update_2004.pdf

Kim NH (2005) Podocyte hypertrophy in diabetic nephropathy. Nephrology (Carlton) 10 Suppl: S14-16

Komeda K, Noda M, Terao K, Kuzuya N, Kanazawa M, Kanazawa Y (1998) Establishment of two substrains, diabetes-prone and non-diabetic, from Long-Evans Tokushima Lean (LETL) rats. Endocr J 45: 737-744

Kramer JW (1981) Animal model of human disease: Inherited early-onset, insulin-requiring diabetes mellitus in keeshond dogs. Am J Pathol 105: 194-196

Kuzuya T, Nakagawa S, Satoh J, Kanazawa Y, Iwamoto Y, Kobayashi M, Nanjo K, Sasaki A, Seino Y, Ito C, Shima K, Nonaka K, Kadowaki T (2002) Report of the Committee on the classification and diagnostic criteria of diabetes mellitus. Diabetes Res Clin Pract 55: 65-85

Leiter EH, Reifsnyder PC (2004) Differential levels of diabetogenic stress in two new mouse models of obesity and type 2 diabetes. Diabetes 53 Suppl 1: S4-11

Lewis JT, Dayanandan B, Habener JF, Kieffer TJ (2000) Glucose-dependent insulinotropic polypeptide confers early phase insulin release to oral glucose in rats: demonstration by a receptor antagonist. Endocrinology 141: 3710-3716

Licht AH, Nübel T, Feldner A, Jurisch-Yaski N, Marcello M, Demicheva E, Hu J, Hartenstein B, Augustin HG, Hecker M, Angel P, Korff T, Schorpp-Kistner M (2010) Junb regulates aterial contraction capacity, cellular contractility, and motility via its target Myl9 in mice. J Clin Invest

Liu B, Preisig PA (2002) Compensatory renal hypertrophy is mediated by a cell cycle-dependent mechanism. Kidney Int 62: 1650-1658

Liu ZC, Chow KM, Chang TM (2003) Evaluation of two protocols of uremic rat model: partial nephrectomy and infarction. Ren Fail 25: 935-943

Marsh SA, Dell'italia LJ, Chatham JC (2009) Interaction of diet and diabetes on cardiovascular function in rats. Am J Physiol Heart Circ Physiol 296: H282-292

Marshall SM (2005) The podocyte: a major player in the development of diabetic nephropathy? Horm Metab Res 37 Suppl 1: 9-16

Marshall T, Williams KM (1998) Clinical analysis of human urinary proteins using high resolution electrophoretic methods. Electrophoresis 19: 1752-1770

Melhem MF, Craven PA, Liachenko J, DeRubertis FR (2002) Alpha-lipoic acid attenuates hyperglycemia and prevents glomerular mesangial matrix expansion in diabetes. J Am Soc Nephrol 13: 108-116

Miralles F, Portha B (2001) Early development of beta-cells is impaired in the GK rat model of type 2 diabetes. Diabetes 50 Suppl 1: S84-88

Miyawaki K, Yamada Y, Yano H, Niwa H, Ban N, Ihara Y, Kubota A, Fujimoto S, Kajikawa M, Kuroe A, Tsuda K, Hashimoto H, Yamashita T, Jomori T, Tashiro F, Miyazaki J, Seino Y (1999) Glucose intolerance caused by a defect in the entero-insular axis: a study in gastric inhibitory polypeptide receptor knockout mice. Proc Natl Acad Sci U S A 96: 14843-14847

Mizuno S, Wen J, Mizuno-Horikawa Y (2004) Repeated streptozotocin injections cause early onset of glomerulosclerosis in mice. Exp Anim 53: 175-180

Mogensen CE, Keane WF, Bennett PH, Jerums G, Parving HH, Passa P, Steffes MW, Striker GE, Viberti GC (1995) Prevention of diabetic renal disease with special reference to microalbuminuria. Lancet 346: 1080-1084

Mohan S, Reddick RL, Musi N, Horn DA, Yan B, Prihoda TJ, Natarajan M, Abboud-Werner SL (2008) Diabetic eNOS knockout mice develop distinct macro- and microvascular complications. Lab Invest 88: 515-528

Mundel P, Shankland SJ (2002) Podocyte biology and response to injury. J Am Soc Nephrol 13: 3005-3015

Nagata M, Kriz W (1992) Glomerular damage after uninephrectomy in young rats. II. Mechanical stress on podocytes as a pathway to sclerosis. Kidney Int 42: 148-160

Nagata M, Scharer K, Kriz W (1992) Glomerular damage after uninephrectomy in young rats. I. Hypertrophy and distortion of capillary architecture. Kidney Int 42: 136-147

Nakayama T, Sato W, Kosugi T, Zhang L, Campbell-Thompson M, Yoshimura A, Croker BP, Johnson RJ, Nakagawa T (2009) Endothelial injury due to eNOS deficiency accelerates the progression of chronic renal disease in the mouse. Am J Physiol Renal Physiol 296: F317-327

Newman DJ, Mattock MB, Dawnay AB, Kerry S, McGuire A, Yaqoob M, Hitman GA, Hawke C (2005) Systematic review on urine albumin testing for early detection of diabetic complications. Health Technol Assess 9: iii-vi, xiii-163

Ninichuk V, Kulkarni O, Clauss S, Anders HJ (2007) Tubular atrophy, interstitial fibrosis, and inflammation in type 2 diabetic db/db mice. An accelerated model of advanced diabetic nephropathy. Eur J Med Res 12: 351-355

Okada T, Omoto-Kitao M, Mukamoto M, Nakamura J, Mino M, Kondo T, Takeshita A, Kusakabe KT, Kato K (2010) Compensatory renal growth in uninephrectomized immature rats: proliferative activity and epidermal growth factor. J Vet Med Sci 72: 975-980

Osterby R, Gall MA, Schmitz A, Nielsen FS, Nyberg G, Parving HH (1993) Glomerular structure and function in proteinuric type 2 (non-insulin-dependent) diabetic patients. Diabetologia 36: 1064-1070

Pagtalunan ME, Miller PL, Jumping-Eagle S, Nelson RG, Myers BD, Rennke HG, Coplon NS, Sun L, Meyer TW (1997) Podocyte loss and progressive glomerular injury in type II diabetes. J Clin Invest 99: 342-348

Parving HH, Hovind P, Rossing K, Andersen S (2001) Evolving strategies for renoprotection: diabetic nephropathy. Curr Opin Nephrol Hypertens 10: 515-522

Pederson RA, Satkunarajah M, McIntosh CH, Scrocchi LA, Flamez D, Schuit F, Drucker DJ, Wheeler MB (1998) Enhanced glucose-dependent insulinotropic polypeptide secretion and insulinotropic action in glucagon-like peptide 1 receptor -/- mice. Diabetes 47: 1046-1052

Preitner F, Burcelin R, Ibberson M, Hansotia T, Drucker D, Thorens B (2002) Disruption of both GLP-1 and GIP signalling pathways in the mouse leads to glucose intolerance. Diabetes 52: Suppl 2, A66

Reddi AS, Camerini-Davalos RA (1990) Diabetic nephropathy. An update. Arch Intern Med 150: 31-43

Reed MJ, Meszaros K, Entes LJ, Claypool MD, Pinkett JG, Gadbois TM, Reaven GM (2000) A new rat model of type 2 diabetes: the fat-fed, streptozotocin-treated rat. Metabolism 49: 1390-1394

Rees DA, Alcolado JC (2005) Animal models of diabetes mellitus. Diabet Med 22: 359-370

Resnick HE, Howard BV (2004) Cardiovascular Disease in Diabetes Encyclopedia of Endocrine Diseases. Elsevier Inc., pp 476-479

Rithidech KN, Cronkite EP, Bond VP (1999) Advantages of the CBA mouse in leukemogenesis research. Blood Cells Mol Dis 25: 38-45

Ritz E (1999) Nephropathy in type 2 diabetes. J Intern Med 245: 111-126

Ritz E (2006) Diabetic nephropathy. Saudi J Kidney Dis Transpl 17: 481-490

Roth SI, Conaway HH (1982) Animal model of human disease. Spontaneous diabetes mellitus in the New Zealand white rabbit. Am J Pathol 109: 359-363

Schmidt RE, Dorsey DA, Beaudet LN, Peterson RG (2003) Analysis of the Zucker Diabetic Fatty (ZDF) type 2 diabetic rat model suggests a neurotrophic role for insulin/IGF-I in diabetic autonomic neuropathy. Am J Pathol 163: 21-28

Schwieger J, Fine LG (1990) Renal hypertrophy, growth factors, and nephropathy in diabetes mellitus. Semin Nephrol 10: 242-253

Scrocchi LA, Brown TJ, MacLusky N, Brubaker PL, Auerbach AB, Joyner AL, Drucker DJ (1996) Glucose intolerance but normal satiety in mice with a null mutation in the glucagon-like peptide 1 receptor gene. Nat Med 2: 1254-1258

Sharma K, McCue P, Dunn SR (2003) Diabetic kidney disease in the db/db mouse. Am J Physiol Renal Physiol 284: F1138-1144

Sowers JR, Epstein M (1995) Diabetes mellitus and associated hypertension, vascular disease, and nephropathy. An update. Hypertension 26: 869-879

Sowers JR, Epstein M, Frohlich ED (2001) Diabetes, hypertension, and cardiovascular disease: an update. Hypertension 37: 1053-1059

Sterio DC (1984) The unbiased estimation of number and sizes of arbitrary particles using the disector. J Microsc 134: 127-136

Sviglerova J, Kuncova J, Nalos L, Tonar Z, Rajdl D, Stengl M (2010) Cardiovascular parameters in rat model of chronic renal failure induced by subtotal nephrectomy. Physiol Res 59 Suppl 1: S81-88

Teiken JM, Audettey JL, Laturnus DI, Zheng S, Epstein PN, Carlson EC (2008) Podocyte loss in aging OVE26 diabetic mice. Anat Rec (Hoboken) 291: 114-121

Tejera N, Gomez-Garre D, Lazaro A, Gallego-Delgado J, Alonso C, Blanco J, Ortiz A, Egido J (2004) Persistent proteinuria up-regulates angiotensin II type 2 receptor and induces apoptosis in proximal tubular cells. Am J Pathol 164: 1817-1826

Tervaert TW, Mooyaart AL, Amann K, Cohen AH, Cook HT, Drachenberg CB, Ferrario F, Fogo AB, Haas M, de Heer E, Joh K, Noel LH, Radhakrishnan J, Seshan SV, Bajema IM, Bruijn JA (2010) Pathologic classification of diabetic nephropathy. J Am Soc Nephrol 21: 556-563

Tesch GH, Allen TJ (2007) Rodent models of streptozotocin-induced diabetic nephropathy. Nephrology (Carlton) 12: 261-266

van Goor H, Fidler V, Weening JJ, Grond J (1991) Determinants of focal and segmental glomerulosclerosis in the rat after renal ablation. Evidence for involvement of macrophages and lipids. Lab Invest 64: 754-765

Volz A (1997) Cloning and functional characterization of the human GIP receptor. Inaugural - Dissertation to achieve the doctor title of biology at the University of Marburg 1-159: 1-159

Wang S, LaPage J, Hirschberg R (2000) Proteinuria and progression of chronic renal disease. Kidney Blood Press Res 23: 167-169

Wanke R (1996) Zur Morpho- und Pathogenese der progressiven Glomerulosklerose. Habilitationsschrift. Ludwig-Maximilians-Universität München. 1-257

Wanke R, Wolf E, Brem G, Hermanns W (2001) [Role of podocyte damage in the pathogenesis of glomerulosclerosis and tubulointerstitial lesions: findings in the growth hormone transgenic mouse model of progressive nephropathy]. Verh Dtsch Ges Pathol 85: 250-256

Wehner H (1983) [Morphology of diabetic microangiopathy of the kidney]. Med Welt 34: 18-19

Weibel ER, Gomez DM (1962) A principle for counting tissue structures on random sections. J Appl Physiol 17: 343-348

Weibel ER (1980) Stereological Methods II. Theoretical foundations. Academic press London

WHO (2009) Diabetes. World health organization Fact sheet N°312, Available from http://www.who.int/mediacentre/factsheets/fs312/en/index.html

Wiggins JE, Goyal M, Sanden SK, Wharram BL, Shedden KA, Misek DE, Kuick RD, Wiggins RC (2005) Podocyte hypertrophy, "adaptation," and "decompensation" associated with glomerular enlargement and glomerulosclerosis in the aging rat: prevention by calorie restriction. J Am Soc Nephrol 16: 2953-2966

Wogensen L, Krag S, Chai Q, Ledet T (2005) The use of transgenic animals in the study of diabetic kidney disease. Horm Metab Res 37 Suppl 1: 17-25

Wolf G (2004) New insights into the pathophysiology of diabetic nephropathy: from haemodynamics to molecular pathology. Eur J Clin Invest 34: 785-796

Yang Y, Santamaria P (2006) Lessons on autoimmune diabetes from animal models. Clin Sci (Lond) 110: 627-639

Zeier M, Geberth S, Gonzalo A, Chauveau D, Grunfeld JP, Ritz E (1992) The effect of uninephrectomy on progression of renal failure in autosomal dominant polycystic kidney disease. J Am Soc Nephrol 3: 1119-1123

Zheng S, Noonan WT, Metreveli NS, Coventry S, Kralik PM, Carlson EC, Epstein PN (2004) Development of late-stage diabetic nephropathy in OVE26 diabetic mice. Diabetes 53: 3248-3257

Ziyadeh FN, Wolf G (2008) Pathogenesis of the podocytopathy and proteinuria in diabetic glomerulopathy. Curr Diabetes Rev 4: 39-45

9. Attachment

9.1 Protocol for silver staining of SDS-PAGE gels

	Silver stain for SDS-PAGE gels	
1.)	**Fixation solution** 99.6 % Ethanol (Roth, Germany) l Glacial acetic acid (Sigma, Germany) 37% Formaldehyde (Roth, Germany) ad 1000 ml distilled water	60 minutes 500 m 120 ml 0.5 ml
2.)	**Washing in 50 % Ethanol**	3 x 20 minutes
3.)	**Pre-treatment** Sodium thiosulphate (Merck, Germany) ad 50 ml distilled water	1 minute 0.05 g
4.)	**Washing in distilled water**	3 x 20 seconds
5.)	**Impregnation** Silver nitrate (Roth, Germany) 37% Formaldehyde (Roth, Germany) ad 50 ml distilled water	20 minutes 0.05 g 35 µl
6.)	**Washing in distilled water**	2x 20 seconds
7.)	**Develop** Sodium carbonate (Roth, Germany) Sodium thiosulphate (Merck, Germany) 37% Formaldehyde (Roth, Germany) ad 1000 ml distilled water	until bands become visible 3 g 0.2 mg 50 µl
8.)	**Washing in distilled water**	20 seconds
9.)	**Stop solution** 0.1 M EDTA (Sigma, Germany)	

9.2 Drying of SDS-PAGE gels

The DryEase™ Mini-Gel Drying System (DryEase Mini-Gel Dryer Frame, DryEase Mini-Gel Drying Base, DryEase Mini Cellophane and Gel-Dry Drying Solution; Novex, Germany) was used for drying polyacrylamid gels. Stained gels were washed in distilled water 3 times for 2 minutes and then equilibrated in Gel-dry Solution for 15-20 minutes on a rotary shaker (Heidolph, Germany). Rough edges of the gel were cut off, using a razor blade. 2 pieces of cellophane were pre-wetted in Gel-Drying Solution for 15-20 seconds. A DryEase gel drying frame was placed on the gel dryer

base and covered with one cellophane piece. The gel was placed in the centre of the cellophane sheet; no air was to be trapped between the gel and the cellophane sheet. The gel was covered with a second layer of pre-wetted cellophane. No air was to be trapped between gel and the cellophane sheets. Wrinkles were removed with a gloved hand. The remaining frame was aligned so that its corner pins fit into the holes on the bottom frame. Plastic clamps were pushed onto the four edges of the frame. The assembly was set upright. Gels were dried for 12-36 hours; drafts were avoided. The gel/cellophane sandwich was removed and excess cellophane was trimmed off. Dried gels were pressed between pages of a book for approximately 2 days and then stored in a cassette.

Perspective

The glomerular basement membrane thickness should be measured, since this is one of the earliest morphological alterations observed in diabetic nephropathy. Calculation of the filtration slit frequency (FSF) of the podocyte foot projections should also be carried out because a reduced FSF in uninephrectomized transgenic mice might explain the higher ACR of these animals vs. sham operated mice.

Since uninephrectomized GIPR^{dn} transgenic diabetic mice serve as a very promising model for the study of diabetic nephropathy, clinical studies on novel diabetes medication should follow uninephrectomy, e.g. Pioglitazon (used for the treatment of type 2 diabetes mellitus), in order to find out if at any time it is possible to intervene and/ or reverse the pathological process.

Further research should pick up molecular mechanisms that aggravate the course towards advanced glomerular lesions in end-stage kidney diseases of the investigated animal model, such as real time PCR of isolated glomeruli to study pathogenic factors.

Acknowledgements

I would like to thank Prof. Dr. Rüdiger Wanke for giving me the opportunity to perform this dissertation. I am extremely grateful for his immense patience and kindness.

I also wish to express my great gratitude to Dr. Nadja Herbach for her generous help in performing this doctorate, her immense support, care, hospitality, guidance, and continuous belief in me.

My special thanks go to Dr. Andreas Blutke, Dr. Lelia van Bürck, Dr. Sabine Kautz, Mrs. Marion Schuster, and Mr. Pierre Börjes for their support and friendship.

Further acknowledgements go to all employees at the Institute of Veterinary Pathology for their help, especially to Mrs. Angela Siebert for her always kind and helpful attitude and dedicated work, Mrs Lisa Pichl for laboratory assistance at all times, Mrs. Beate Schmidt, and Mrs. Marjam O'Gorman for their encouragement and company, Mrs. Sabine Zwirz and Mr. Adrian Ciolovan for animal care, Mrs. Heike Sperling for performance of plastic histology. A special thank goes to the staff of the laboratory of the Clinic for Internal Veterinary Medicine (Head: Prof. Dr. Katrin Hartmann) for measurement of the creatinine contents in the urine samples, and to the staff of the City Clinic Munich in Schwabing for screening of the serum parameters.

Finally, I am particularly grateful to my loving family, my wonderful husband and my dear friends, especially to *Elisabeth Albescu*, for always being there for me, supporting me, and never loosing their faith in me.